NASA TECHNICAL MEMORANDUM

NASA TM X-3565

NASA TM X-3565

USERS' MANUAL FOR COMPUTER PROGRAM FOR ONE-DIMENSIONAL ANALYSIS OF COUPLED-CAVITY TRAVELING WAVE TUBES

Thomas A. O'Malley and Denis J. Connolly

Lewis Research Center

Cleveland, Ohio 44135

NATIONAL AERONAUTICS AND SPACE ADMINISTRATION • WASHINGTON D. C. • AUGUST 1977

1. Report No. NASA TM X-3565	2. Government Accession No.	3. Recipient's Catalog No.
4. Title and Subtitle USERS' MANUAL FOR COMPUTER PROGRAM FOR ONE-DIMENSIONAL ANALYSIS OF COUPLED-CAVITY TRAVELING WAVE TUBES		5. Report Date August 1977
		6. Performing Organization Code
7. Author(s) Thomas A. O'Malley and Denis J. Connolly		8. Performing Organization Report No. E-8900
		10. Work Unit No. 506-20
9. Performing Organization Name and Address National Aeronautics and Space Administration Lewis Research Center Cleveland, Ohio 44135		11. Contract or Grant No.
		13. Type of Report and Period Covered Technical Memorandum
12. Sponsoring Agency Name and Address National Aeronautics and Space Administration Washington, D.C. 20546		14. Sponsoring Agency Code
15. Supplementary Notes		

16. Abstract

The use of the coupled-cavity traveling wave tube for space communications has led to an increased interest in improving the efficiency of the basic interaction process in these devices through velocity resynchronization and other methods. To analyze these methods, we have recently developed a flexible, large-signal computer program for use on the IBM 360/67 time-sharing system. The present report is a users' manual for this program.

17. Key Words (Suggested by Author(s)) Traveling wave tubes; Computerized simulation; Electron trajectories		18. Distribution Statement Unclassified - unlimited; STAR Category 32	
19. Security Classif. (of this report) Unclassified	20. Security Classif. (of this page) Unclassified	21. No. of Pages 66	22. Price* A04

* For sale by the National Technical Information Service, Springfield, Virginia 22161

CONTENTS

USERS' MANUAL FOR COMPUTER PROGRAM FOR ONE-DIMENSIONAL ANALYSIS OF COUPLED-CAVITY TRAVELING WAVE TUBES

by Thomas A. O'Malley and Denis J. Connolly

Lewis Research Center

SUMMARY

The use of the coupled-cavity traveling wave tube (TWT) for space communications has led to an increased interest in the efficiency of these devices. Efficiency improvements have generally been along two lines: (1) the development of efficient multistage depressed collectors to recover a high percentage of the kinetic power in the spent beam; and (2) improvements in the efficiency of the basic interaction process through velocity resynchronization and other methods. To pursue the second line, we have recently developed a flexible, large-signal computer program written in FORTRAN IV for use on the IBM 360/67 time-sharing system. The present report is a users' manual for this program.

The basic programming approach consists of dividing the beam into disks and calculating the trajectories of these disks as they pass through a sequence of cavities each of which may have different geometrical and electrical properties. Extreme flexibility is provided in the variety of tube features that can be modeled since each cavity has individually entered input parameters. The program can handle lumped or distributed severs, input and output couplers, cavity match details provided for cavities near the end of a stack, voltage-jump velocity resynchronization with an arbitrary number of discrete steps (up to one per cavity), and velocity taper designs of almost arbitrary complexity. Backward waves can be handled by an iterative procedure.

INTRODUCTION

The use of the coupled-cavity traveling wave tube (TWT) for space communications has led to an increased interest in the efficiency of these devices. Efficiency improvements have generally been along two lines: (1) the development of efficient multistage

depressed collectors to recover a high percentage of the kinetic power in the spent beam (ref. 1); and (2) improvements in the efficiency of the basic interaction process through velocity resynchronization and other methods (ref. 2). The NASA Lewis Research Center has been interested in the first approach to efficiency enhancement for some time (refs. 1 and 3). In order to pursue the second, we have recently developed a flexible, large-signal computer program written in FORTRAN IV for use on the IBM 360/67 time-sharing system (ref. 4). The present report is a users' manual for this program.

The basic programming approach generally follows that described by Vaughan (ref. 5), wherein a disk-model beam is followed through a sequence of cavities each of which may have different geometrical and electrical properties. Extreme flexibility is provided in the variety of tube features that can be modeled since each cavity has individually entered input parameters. The program can handle lumped or distributed severs, input and output couplers, cavity match details provided for cavities near the end of a stack, voltage-jump velocity resynchronization with an arbitrary number of discrete steps (up to one per cavity), and velocity taper designs of almost arbitrary complexity. Backward waves can be handled by an iterative procedure similar to that described by Kino, et al. (ref. 6). The program has been used to analyze the beam-circuit interaction in the 200-watt TWT used on the Communications Technology Satellite. The computer results showed excellent agreement with experimental data.

In this report, we first discuss the computer model of the coupled-cavity TWT. A detailed discussion of the program structure follows. The input data, output data, program variables, and program subroutines are then described. Symbols are defined in appendix A, and a sample problem is given in appendix B.

MODEL OF COUPLED-CAVITY TRAVELING WAVE TUBE

The model of a coupled-cavity TWT is illustrated in figure 1. The beam is treated as a series of rigid but mutually penetrable disks. A complete description of the beam trajectory is obtained by following the disks contained in a single beam wavelength (ref. 7). The number of disks per beam wavelength is an adjustable input parameter but is usually set equal to 24. The diameter of a beam disk (2b in fig. 1) is allowed to take on as many as three different values during the course of a calculation. This option is provided to accommodate the fact that TWT beams tend to expand in the saturation region of the tube. The beam may expand until some portion of it is intercepted by the tunnel wall. To accommodate this interception, the program allows the disks to lose some portion of their charge and mass at specified points along the tube.

The tube body is treated as a conducting tunnel of radius a divided axially into a

series of discrete cells, where the length of the k^{th} cell is denoted by L_k. In the center of each cell is a gap of length $2l_k$. Impressed across the k^{th} gap is a complex voltage $V_k e^{i\omega t}$.

In the absence of a beam, there will be a simple known relation among the various V_k. For a forward-propagating wave in the pass band of a uniform structure,

$$V_{k+1} = e^{-(\alpha + i\beta_1)L_k} V_k \qquad (1)$$

where α and β_1 are known from cold-test measurements. The power flowing along the structure will be given by

$$P_k = \frac{|V_k|^2}{2Z_k} \qquad (2)$$

where Z_k also is known from cold-test measurements.

The voltage wave in the presence of the beam is calculated by adding a complex induced voltage to the propagating wave, that is,

$$V_{k+1} = e^{-(\alpha + i\beta_1)L_k} V_k + \Delta V_{k+1} \qquad (3)$$

where ΔV_{k+1} is an induced voltage to be defined later.

The body of a coupled-cavity TWT is supposedly a periodic structure. If this were the case, all cavities would have the same L, l, αL, $\beta_1 L$, and Z. However, a real tube has input and output couplers, severs, and perhaps velocity tapers and cavity match details, all of which require individual nonperiodic treatment in the model. Thus, the properties of individual cavities are separately specified input parameters in the program, and a great variety of tube design variations such as complicated velocity tapers or voltage-jump configurations can be easily modeled. Equation (3) is easily modified to handle such a quasi-periodic structure,

$$V_{k+1} = \tau_k \sqrt{\frac{Z_{k+1}}{Z_k}}\, V_k + \Delta V_{k+1}$$

where

$$\tau_k = e^{-(\alpha L)_k - i(\beta_1 L)_k}$$

The factor $\sqrt{Z_{k+1}/Z_k}$ ensures that power flow is conserved.

PROGRAM STRUCTURE

The program consists of two major elements: the dynamics of the beam disks and the beam-wave coupling analysis. These two elements are described in detail in the following sections.

Dynamics of Beam Disks

The computational problem discussed in this section is the calculation of beam disk trajectories in a suitable manner. Ordinarily, the computational procedure is to first solve for the disk acceleration. Numerical integration of this equation then yields $v_i(t)$, the velocity of the i^{th} disk at time t. Numerical integration of $v_i(t)$ yields $z_i(t)$, the axial position of the i^{th} disk at time t.

Instead of using the functions $v_i(t)$ and $z_i(t)$ to describe the trajectories, it is more convenient for our purposes to let z be the independent variable and to calculate the functions $dt_i(z)/dz$ and $t_i(z)$. Here $dt_i(z)/dz$ is the reciprocal of the velocity of the i^{th} disk when it reaches the axial position z, and $t_i(z)$ is the time of arrival of the i^{th} disk at the axial position z. In terms of these new functions, the equations of motion are

$$\frac{d^2 t_i}{dz^2} = \frac{-F_{zi}}{m_d}\left[1 - \frac{1}{\left(\frac{dt_i}{dz} c\right)^2}\right]^{3/2} \left(\frac{dt_i}{dz}\right)^3 \qquad i = 1, \ldots, N_d \tag{4}$$

where F_{zi} is the total axial force on the i^{th} disk, c is the velocity of light, m_d is the rest mass of a disk, and N_d is the number of disks.

Instead of using t_i and z we use the normalized variables θ_i and ξ defined by

$$\theta_i = \omega t_i$$

and

$$\xi = \frac{z}{a}$$

where ω is the angular frequency and a is the tunnel radius. These normalized variables are used in the program. At times, however, greater clarity in the explanation of a topic can be achieved by using the unnormalized variables t_i and z. At such times in this report, the unnormalized variables are used. In terms of the normalized variables, the equations of motion are

$$\frac{d^2\theta_i}{d\xi^2} = \frac{-F_{zi}}{m_d a\omega^2}\left[1 - \frac{1}{\left(\frac{d\theta_i}{d\xi}\frac{c}{\omega a}\right)^2}\right]^{3/2}\left(\frac{d\theta_i}{d\xi}\right)^3 \qquad i = 1, \ldots, N_d \tag{5}$$

The initial conditions are

$$\frac{d\theta_i}{d\xi} = \frac{\omega a}{u_0} \qquad i = 1, \ldots, N_d$$

$$\theta_i = \frac{(i - 1)\omega l_d}{u_0} \qquad i = 1, \ldots, N_d$$

where l_d is the axial length of a disk and u_0 is the initial beam velocity, given by

$$u_0 = c\sqrt{1 - \frac{1}{\left(1 + \frac{q_d V_0}{m_d c^2}\right)^2}}$$

In this equation, V_0 is the beam accelerating voltage and q_d is the charge of a disk.

The coordinate system used in the program has its origin at the beginning of the first cavity. The k^{th} cavity is divided into N_z equal parts of length Δz_k, given by

$$\Delta z_k = \frac{L_k}{N_z}$$

The n^{th} node in the first cavity, denoted by z_{n1}, is defined by

$$z_{n1} = \left(n - \frac{1}{2}\right)\Delta z_1 \qquad n = 1, \ldots, N_z \tag{6}$$

The n^{th} node in the k^{th} cavity, denoted by z_{nk}, is given by

$$z_{nk} = \sum_{m=1}^{k-1} L_m + \left(n - \frac{1}{2}\right)\Delta z_k \qquad n = 1, \ldots, N_z;\; k = 2, \ldots, N_c \tag{7}$$

where N_c is the number of cavities. A point that lies midway between two nodes $z_{n,k}$ and $z_{n+1,k}$ is denoted by $z_{n+\frac{1}{2},k}$. Such a point is called the n^{th} antinode in cavity k (fig. 2). The numerical integration of equation (4) is such that the functions dt_i/dz and $t_i(z)$ are evaluated at antinodes and the functions d^2t_i/dz^2 are evaluated at nodes.

At some point in cavity k, we have trajectory data at node $n - 1$ and antinode $n - 1$; that is, the functions $d^2t_i(z_{n-1,k})/dz^2$, $dt_i(z_{n-\frac{1}{2},k})/dz$, and $t_i(z_{n-\frac{1}{2},k})$ are known. The problem now is to obtain $d^2t_i(z_{nk})/dz^2$, $dt_i(z_{n+\frac{1}{2},k})/dz$, and $t_i(z_{n+\frac{1}{2},k})$. We first obtain approximations for $dt_i(z_{nk})/dz$ and $t_i(z_{nk})$ with the equations

$$\frac{dt_i(z_{nk})}{dz} = \frac{dt_i(z_{n-\frac{1}{2},k})}{dz} + \frac{d^2t_i(z_{n-1,k})}{dz^2}\,\frac{\Delta z_k}{2} \tag{8}$$

$$t_i(z_{nk}) = t_i(z_{n-\frac{1}{2},k}) + \frac{dt_i(z_{n-\frac{1}{2},k})}{dz}\,\frac{\Delta z_k}{2} + \frac{1}{2}\,\frac{d^2t_i(z_{n-1,k})}{dz^2}\left(\frac{\Delta z_k}{2}\right)^2 \tag{9}$$

Knowing, at least approximately, $dt_i(z_{nk})/dz$ and $t_i(z_{nk})$, we can evaluate $d^2t_i(z_{nk})/dz^2$ from equation (4). We now obtain $dt_i(z_{n+\frac{1}{2},k})/dz$ and $t_i(z_{n+\frac{1}{2},k})$ by the equations

$$\frac{dt_i(z_{n+\frac{1}{2},k})}{dz} = \frac{dt_i(z_{n-\frac{1}{2},k})}{dz} + \frac{d^2t_i(z_{nk})}{dz^2}\Delta z_k \tag{10}$$

$$t_i(z_{n+\frac{1}{2},k}) = t_i(z_{n-\frac{1}{2},k}) + \frac{dt_i(z_{n-\frac{1}{2},k})}{dz}\Delta z_k + \frac{1}{2}\frac{d^2t_i(z_{nk})}{dz^2}\Delta z_k^2 \tag{11}$$

Space charge forces. - The space charge force on one disk of radius b due to another disk of radius b, with a separation distance of z, is given by (ref. 4, eq. (13))

For $|z| > l_d$:

$$F = \frac{4a^2q_d^2\,\mathrm{sgn}(z)}{(l_d')^2 b^2 \pi\epsilon_0}\sum_{m=1}^{\infty}\frac{\left[J_1\left(\frac{\lambda_m b}{a}\right)\right]^2}{\lambda_m^4\left[J_1(\lambda_m)\right]^2}\left[\cosh\left(\frac{\lambda_m l_d'}{a}\right) - 1\right]e^{-\lambda_m|z'|/a} \tag{12}$$

For $|z| < l_d$:

$$F = \frac{4a^2q_d^2\,\mathrm{sgn}(z)}{(l_d')^2 b^2 \pi\epsilon_0}\sum_{m=1}^{\infty}\frac{\left[J_1\left(\frac{\lambda_m b}{a}\right)\right]^2}{\lambda_m^4\left[J_1(\lambda_m)\right]^2}\left(1 - e^{-\lambda_m|z'|/a} - e^{-\lambda_m l_d'/a}\sinh\lambda_m\frac{|z'|}{a}\right) \tag{13}$$

where J_1 is the Bessel function of order 1, λ_m is the m^{th} zero of the Bessel function of order zero, ϵ_0 is the permittivity of free space, and l_d' and z' are given by

$$l_d' = \frac{l_d}{\sqrt{1 - \left(\frac{u_0}{c}\right)^2}}$$

$$z' = \frac{z}{\sqrt{1 - \left(\frac{u_0}{c}\right)^2}}$$

The function F defined in equations (12) and (13) is continuous for all values of z. In particular, there is no jump discontinuity at $z = 0$.

Using equations (12) and (13) for calculating space charge forces on each integration step would be intolerably slow. The method used herein is to set up N_b tables corresponding to the N_b discrete disk diameters. Each table contains 100 data points corresponding to 100 separation distances. The n^{th} data point would be the space charge force between two disks, as calculated by equation (12) or (13), separated by the n^{th} separation distance. In the computer simulation, the space charge force on one disk due to another is calculated by using linear interpolation on the appropriate table. If the two disks in question have different diameters, two linear interpolations are done on the appropriate tables, and the average is taken.

Fortunately, the space charge force on a given disk is a slowly varying function of the independent variable z. This is especially true in the beginning cavities of the tube. To take advantage of the slowly varying nature of the space charge force, the calculation is not done on every integration step. The calculation of space charge forces is initially done every N^{th} step, where N is an input. The value of N may change during the simulation in a manner to be described later. On those integration steps where space charge forces are not calculated, they are approximated by quadratic curve fits. Each disk has its own curve fit. These curve fits are obtained by fitting a quadratic polynomial through the latest three calculations of space charge forces. Let us say that these three calculations were done when z was equal to z_a, z_b, and z_c. At an integration step where a new space charge force calculation is due, at $z = z_d$, the values calculated are compared with those obtained when the curve fits based on the points z_a, z_b, and z_c are evaluated at z_d. If the difference in the values for any disk is exceeded by a specified tolerance, the next calculation of space charge forces occurs $\frac{1}{2}N$ steps later. In general, N is halved each time the specified tolerance is exceeded.

For calculating space charge forces, the positions of all disks must be known at a time t. This information is not readily available since z rather than t is the inde-

pendent variable. To calculate the space charge force on the i^{th} disk located at some z, we must determine the positions of all the other disks at the time $t_i(z)$. Consider the j^{th} disk. The time of arrival $t_j(z)$ at z is known. By the periodicity of the motion, the disk that originally was m wavelengths behind the j^{th} disk arrives at z at the time $t_j(z) + mT$, where T is the reciprocal of frequency. Similarly, the disk that originally was m wavelengths ahead of the j^{th} disk arrives at z at the time $t_j(z) + (-m)T$. We consider all such disks and find m such that

$$|t_i(z) - (t_j(z) + mT)| = \text{Minimum} \tag{14}$$

We may call the disk in question the j^{th} disk in the m^{th} cycle. If the input parameter KCYCLE is zero, we assume that the j^{th} disk in any other cycle is too far away from the i^{th} disk, at the time $t_i(z)$, to contribute significantly to the space charge force on the i^{th} disk. If KCYCLE is not zero, we also consider the j^{th} disk in cycles $m - 1$ and $m + 1$. Let z_j^m be the position of the j^{th} disk in the m^{th} cycle at the time $t_i(z)$. We obtain z_j^m by assuming that this disk has constant velocity $v_j(z)$ in the time interval spanned by $t_i(z)$ and $t_j(z) + mT$. Then z_j^m is given by

$$z_j^m = z + v_j(z)\left[t_i(z) - (t_j(z) + mT)\right] \tag{15}$$

Similar expressions are obtained, if required, for z_j^{m-1} and z_j^{m+1}. The space charge force is then calculated based on the separation distance $z - z_j^m$. The calculation is done for all disks, excluding the i^{th} disk, and the results are summed to obtain the total space charge force on the i^{th} disk. When the separation distance $z - z_j^m$ is greater than a specified value, the space charge calculation is not done for this term in the summation.

Radiofrequency electric field forces. - Forces on a disk are always evaluated when the disk is at a node. This follows from equation (4) and the fact that d^2t_i/dz^2 is always evaluated at a node. So consider a disk in the k^{th} cavity located at the n^{th} node z_{nk}. The axial force on the disk due to the radiofrequency (rf) electric field, at time t, is given by (ref. 4, eq. (20))

$$F_{rf} = \frac{q_d \mu}{L_k \ell_k \sinh\mu} \sum_{m=-\infty}^{\infty} \frac{C_{mk} I_1(\gamma_{mk} b_k)}{\gamma_{mk} b_k I_0(\gamma_{mk} a)} \frac{\sin\frac{\beta_{mk}\ell_d}{2}}{\beta_{mk}\frac{\ell_d}{2}} \operatorname{Re}\left[\left(V_{fk}\, e^{-i\beta_{mk} y_{nk}} + V_{bk}\, e^{i\beta_{mk} y_{nk}}\right) e^{i\omega t}\right] \tag{16}$$

where

$$C_{mk} = \frac{2l_k(\mu \sinh \mu \cos \beta_{mk}l_k + \beta_{mk}l_k \cosh \mu \sin \beta_{mk}l_k)}{\mu^2 + (\beta_{mk}l_k)^2} \tag{17}$$

$$\beta_{mk} = \beta_{0k} + \frac{2m\pi}{L_k} \tag{18}$$

$$\gamma_{mk} = \sqrt{\beta_{mk}^2 - \left(\frac{\omega}{c}\right)^2} \tag{19}$$

$$y_{nk} = z_{nk} - \left(\sum_{m=1}^{k-1} L_m + \frac{L_k}{2}\right) \tag{20}$$

In equation (16), V_{fk} is the forward-traveling voltage and V_{bk} is the backward-traveling voltage for the k^{th} cavity. In equations (16) and (17), μ is a shaping factor that is chosen to best suit the geometry of the gap. In the case of very blunt tunnel tips, $\mu = 0$. In equation (18), β_{0k} is the lowest order phase shift for the k^{th} cavity. In equation (20), y_{nk} is the axial position, relative to the center of the k^{th} cavity, of the n^{th} node in the cavity.

We define Q_{nk} by

$$Q_{nk} = \frac{q_d\mu}{L_k l_k \sinh(\mu)} \sum_{m=-\infty}^{\infty} \frac{C_{mk} I_1(\gamma_{mk} b_k)}{\gamma_{mk} b_k I_0(\gamma_{mk} a)} \left(\frac{\sin \frac{\beta_{mk} l_d}{2}}{\frac{\beta_{mk} l_d}{2}}\right) e^{-i\beta_{mk} y_{nk}}$$

$$n = 1, \ldots, N_z; \; k = 1, \ldots, N_c \tag{21}$$

Then the electric field force on the i^{th} disk located at z_{nk} is given by

$$F_{ink} = \mathrm{Re}\left[\left(Q_{nk}V_{fk} + Q_{nk}^{*}V_{bk}\right)e^{i\omega t_i(z_{nk})}\right] \tag{22}$$

The Q_{nk} are calculated and stored in a table when cavity k is entered. The number of terms included in the summation is determined by an input parameter. If the number of terms in the summation is no larger than about 40, the computer time for calculating the table is small compared with the total computer time. If cavity k has the same L_k, l_k, β_{0k}, and b_k as cavity $k - 1$, then $Q_{n,k-1} = Q_{nk}$ and a new table does not have to be calculated. When a new table does have to be calculated, the old table is no longer needed, and the new table may occupy the same storage space as the old table. The electric field force is evaluated by equation (22).

Voltage-jump electric field forces. - Consider a disk in the k^{th} cavity located at the n^{th} node z_{nk}. Let V_{Jk} be the voltage jump associated with cavity k. Then the electric field force on the disk is given by (ref. 4, eq. (31))

$$F_{nk} = R_{nk} V_{Jk}$$

where R_{nk} is given by

$$R_{nk} = -\frac{q_d}{L_k}\left\{1 + \frac{2\mu}{l_k \sinh\mu} \sum_{m=1}^{\infty} \frac{C_{mk} I_1(k_m b_k) \sin\left(\frac{k_m l_d}{2}\right) \cos k_m y_{nk}}{k_m b_k I_0(k_m a)\left(\frac{k_m l_d}{2}\right)}\right\}$$

$$|y_{nk}| \leq \frac{L_k - l_d}{2} \tag{23}$$

$$R_{nk} = \frac{-q_d}{L_k}\left\{\frac{L_k + l_d - 2|y_{nk}|}{2l_d} + \frac{\mu}{l_k \sinh\mu} \sum_{m=1}^{\infty} \frac{C_{mk} I_1(k_m b_k) \sin\left(\frac{k_m l_d}{2} - k_m|y_{nk}|\right)}{k_m b_k I_0(k_m a)\left(\frac{k_m l_d}{2}\right)}\right\}$$

$$\frac{L_k - l_d}{2} \leq |y_{nk}| \leq \frac{L_k + l_d}{2} \tag{24}$$

where k_m is given by

$$k_m = \frac{2m\pi}{L_k} \tag{25}$$

The R_{nk} are calculated and stored in a table and have the same features as the Q_{nk} for rf electric field forces.

Beam-Wave Coupling Analysis

The parameters of interest in the beam-wave interaction in the k^{th} cavity are the forward induced voltage ΔV_{fk} and the backward induced voltage ΔV_{bk}. First, we define the fundamental Fourier component of the current density by

$$J_1(z) = \frac{1}{T} \int_0^T J_z(z, t') e^{-i\omega t'} \, dt'$$

It can be shown (ref. 4, eq. (81)) that $J_1(z)$ is given by

$$J_1(z) = \frac{q_d}{\pi b^2 T} \sum_{i=1}^{N_d} \frac{\sin\left[\frac{\omega l_d}{2v_i(z)}\right]}{\left[\frac{\omega l_d}{2v_i(z)}\right]} e^{-i\omega t_i(z)} \tag{26}$$

where N_d is the number of disks. The induced voltages for the k^{th} cavity are then given by (ref. 4, eqs. (75) to (77))

$$\Delta V_{fk} = \int_{-L_k/2}^{L_k/2} \sum_{m=-\infty}^{\infty} P_{mk} \, e^{i\beta_{mk} y} J_1(y) \, dy \tag{27}$$

$$\Delta V_{bk} = \int_{-L_k/2}^{L_k/2} \sum_{m=-\infty}^{\infty} P_{mk}\, e^{-i\beta_{mk} y}\, J_1(y)\, dy \tag{28}$$

where P_{mk} is given by

$$P_{mk} = \frac{\pi \mu b_k C_{mk} Z_k I_1(\gamma_{mk} b_k)}{l_k L_k \sinh(\mu) \gamma_{mk} I_0(\gamma_{mk} a)}$$

In these equations, the integration variable y is the axial position relative to the center of cavity k. The integrals in equations (27) and (28) are evaluated using Simpson's rule with end corrections. The end corrections were derived with the assumption that the number of nodes per cavity N_z is a multiple of four. The results are

$$\Delta V_{fk} = \Delta z_k \sum_{n=1}^{N_z} \delta_n \sum_{m=-\infty}^{\infty} P_{mk}\, e^{i\beta_{mk} y_{nk}}\, J_1(z_{nk}) \tag{29}$$

$$\Delta V_{bk} = \Delta z_k \sum_{n=1}^{N_z} \delta_n \sum_{m=-\infty}^{\infty} P_{mk}\, e^{-i\beta_{mk} y_{nk}}\, J_1(z_{nk}) \tag{30}$$

where, from Simpson's rule with end corrections, the δ_n are

$$\left.\begin{aligned}
&\delta_1 = \frac{1}{3} + \frac{17}{24} && \delta_n = \frac{2}{3},\ 4 \le n \le N_z-2, \text{ if } n \text{ is odd} \\
&\delta_2 = \frac{4}{3} - \frac{7}{24} && \delta_{N_z-1} = \frac{1}{3} + \frac{9}{24} \\
&\delta_3 = \frac{2}{3} + \frac{2}{24} && \delta_{N_z} = \frac{27}{24} \\
&\delta_n = \frac{4}{3},\ 4 \le n \le N_z-2, \text{ if } n \text{ is even} &&
\end{aligned}\right\} \tag{31}$$

We define S_{nk} by

$$S_{nk} = \sum_{m=-\infty}^{\infty} P_{mk} \, e^{i\beta_{mk} y_{nk}} \tag{32}$$

The S_{nk} are calculated and stored in a table that has the same features as the Q_{nk} and R_{nk} tables. Our final expressions for ΔV_{fk} and ΔV_{bk} are

$$\Delta V_{fk} = \Delta z_k \sum_{n=1}^{N_z} \delta_n S_{nk} J_1(z_{nk}) \tag{33}$$

$$\Delta V_{bk} = \Delta z_k \sum_{n=1}^{N_z} \delta_n S_{nk}^{*} J_1(z_{nk}) \tag{34}$$

Calculating the effects of the backward wave requires an iterative procedure. In the first pass through the tube, the ΔV_{bk} are calculated and stored for each cavity k. From the ΔV_{bk}, the backward voltages for a cavity chain from cavity k1 to cavity k2 are obtained from

$$V_{b,k2} = \Delta V_{b,k2} \tag{35}$$

$$V_{bk} = \Delta V_{bk} + V_{b,k+1} \sqrt{\frac{Z_k}{Z_{k+1}}} \, e^{-(\alpha L)_{bk}} \, e^{-i(\beta_1 L)_k} \qquad k = k2 - 1, \ldots, k1 \tag{36}$$

By a cavity chain, we mean a sequence of consecutive cavities whose backward voltages are to be calculated. After V_{bk} are known for the desired cavities, a second pass is made through the tube. The second pass yields a new set of ΔV_{bk} that can be used for calculating a set of V_{bk} for a third pass. The process continues until convergence is obtained. In many applications the iterative procedure will converge faster if the iteration is done on one cavity chain at a time. This would be true, for example, for a tube having severs. The program has the capability of performing the iterative procedure for an arbitrary set of cavity chains.

The computational procedure in the beam-wave interaction process is as follows:

(1) When cavity k is entered, calculate and store the summation S_{nk} in equation (32) for each node n. If cavity k has the same L_k, l_k, β_{0k}, and b_k as cavity $k-1$, then $S_{nk} = S_{n,k-1}$ and a new table does not have to be calculated.

(2) Obtain a first approximation to ΔV_{fk} by assuming that the disks have constant velocity in cavity k. Thus,

$$t_i(z_{nk}) \approx t_i(z_{1k}) + \frac{dt_i(z_{1k})}{dz}(z_{nk} - z_{1k}) \qquad n = 1, \ldots, N_z \tag{37}$$

Knowing $t_i(z_{nk})$, we can calculate $J_1(z_{nk})$ from equation (26) and then calculate ΔV_{fk} from equation (33).

(3) Let the forward voltage for cavity k be

$$V_{fk} = \sqrt{\frac{Z_k}{Z_{k-1}}}\, V_{f,k-1}\, e^{-(\alpha L)_{f,k-1}}\, e^{-i(\beta_1 L)_{k-1}} + \Delta V_{fk} \tag{38}$$

If there is a backward voltage, we assume it is known from equation (36) using the set of ΔV_{bk} obtained from the previous pass through the tube.

(4) Proceed with numerical integration of the equations of motion to obtain trajectory data at each node and antinode in the cavity.

(5) At the n^{th} node in the cavity, after $t_i(z_{nk})$ has been obtained, calculate and store $\delta_n S_{nk} J_1(z_{nk})$ and $\delta_n S_{nk}^* J_1(z_{nk})$. These quantities are the n^{th} terms in the summations of equations (33) and (34).

(6) When the last integration step in cavity k has been done, calculate a better approximation to ΔV_{fk} from equation (33). The ΔV_{fk} so obtained replaces the old ΔV_{fk} calculated in step 2. Also, calculate ΔV_{bk} from equation (34). The ΔV_{bk} are stored for use in the next pass through the tube.

(7) If additional accuracy is required, make another pass through the cavity, repeating steps 3 to 6.

(8) Repeat steps 1 to 7 for cavity $k+1$.

(9) When the last cavity is done and the effects of the backward wave have to be determined, make a second pass through the tube. The backward voltages for the second pass are determined from the ΔV_{bk} of the first pass.

(10) Make as many passes through the tube as are required to obtain convergence.

Summary of Program Steps

The entire computational procedure is given in flow chart form in figure 3. The procedure is summarized by the following steps:

(1) Read input data.

(2) Calculate the tables for space charge forces.

(3) Begin numerical integration of equations of motion with z as the independent variable.

(4) When a new cavity is entered, let us say the k^{th} cavity, print data for cavity $k - 1$. If the parameters of cavity k are different from those of cavity $k - 1$, calculate the tables that are required for evaluation of rf forces, voltage-jump forces, and induced voltages. Obtain a first approximation to ΔV_{fk} by assuming that the disks have constant velocity throughout cavity k. Attenuate and phase shift $V_{f,k-1}$ and vectorially add the result to ΔV_{fk} to obtain the forward voltage for cavity k.

(5) When the last integration step in cavity k has been done, calculate a better approximation to ΔV_{fk}, and use the new approximation in place of the old. Also, calculate and store ΔV_{bk}.

(6) If additional accuracy is required, make a second pass through cavity k.

(7) Repeat from step 4 for cavity $k + 1$.

(8) If the effects of the backward wave are to be determined, make a second pass through the tube.

(9) Make as many passes through the tube as are required to obtain convergence.

DESCRIPTION OF INPUT DATA

The following input data are required by the program:

Name	Symbol	Description
ACM	a	Tunnel radius, cm
ALPHL(K)	$(\alpha L)_{fk}$	Voltage attenuation of forward wave in going from cavity k to cavity $k + 1$, dB per cavity; $k = 1$, LASTCV
ALPHLR(K)	$(\alpha L)_{bk}$	Voltage attenuation of backward wave in going from cavity $k + 1$ to cavity k, dB per cavity; $k = 1$, LASTCV (ALPHLR(K) needs to be loaded only if KLOSS = 1.)

Name	Symbol	Description
B1LDP(K)	$\frac{(\beta_1 L)_k}{\pi}$	Phase shift of voltage for cavity k; k = 1, LASTCV
BCM(I)	b	I^{th} beam radius, cm; I = 1, NUMB (See NUMB, NB1, and NB2 for related inputs.)
COSHML	cosh (μ)	Shaping parameter for electric field $$\frac{E_z(a, z) \text{ at gap edge}}{E_z(a, z) \text{ at gap center}} = \cosh(\mu)$$
DATTEN(I)		In I^{th} interception region, the charge (mass) of a disk is the product of DATTEN(I) and the initial charge (mass); I = 1, NUMA. The interception region is a region throughout which the charge (mass) of a disk is constant. DATTEN(1) is unity and must be loaded. (See NUMA, NA1, and NA2 for related inputs.)
FREQGH	f	Frequency, GHz
I0BMA	I_0	Beam current at tube entrance, mA
INITCV		Number of first cavity considered in the present case
ISAVE		ISAVE = I1 + I2 + I3, where I1, I2, and I3 are defined as follows: I1 = 0: No action I1 = 1: Initial state of the present case will be stored in COMMON/STATE/ for use in a future case. I2 = 0: No action I2 = 2: Initial state of the present case will be stored in a specified data set. I3 = 0: No action I3 = 4: Final state of the present case will be stored in a specified data set.

Name	Symbol	Description
ISTATE		Used only when INITCV $\neq$ 1: ISTATE = 1: Initial state of present case is equal to initial state of previous case. ISTATE = 2: Initial state of present case is equal to final state of previous case. ISTATE = 3: Initial state of present case is equal to initial state of the last case for which I1 (see ISAVE) was equal to 1. ISTATE = 4: Initial state of present case is equal to the state stored in a specified data set.
JSCF		Initially, space charge forces are evaluated once every JSCF steps.
KCYCLE		KCYCLE = 0: Consider only one rf cycle in calculating space charge forces. KCYCLE $\neq$ 0: Consider three rf cycles in calculating space charge forces.
KIMP		KIMP = 0: Pierce impedance is entered as input. KIMP = 1: Total impedance is entered as input. (See ZIMP for related input.)
KLOSS		KLOSS = 0: ALPHLR(K) will be set equal to ALPHL(K); thus, ALPHLR(K) does not need to be loaded. KLOSS = 1: ALPHLR(K) has to be loaded.
KPLOT		KPLOT = 0: Plots are desired. KPLOT $\neq$ 0: Plots are not desired.
KPRINT		KPRINT = 0: Print input data. KPRINT $\neq$ 0: Do not print input data.
KREL		KREL = 0: Use relativistic equations of motion. KREL $\neq$ 0: Use nonrelativistic equations of motion.

Name	Symbol	Description
KSMSIG		KSMSIG = 0: Print small-signal parameters. KSMSIG ≠ 0: Do not print small-signal parameters.
KSPACE		KSPACE = 0: Calculate space charge forces. KSPACE ≠ 0: Set space charge forces equal to zero.
KVEL(I)		Number of cavity for the I^{th} printout of disk velocities; I = 1, NVEL (See NVEL for related input.)
LASTCV		Number of last cavity considered in the present case; LASTCV ≤ 650
LCIRCM(K)	L_k	Length of k^{th} cavity, cm; k = 1, LASTCV
LGAPCM(K)	$2l_k$	Length of k^{th} gap, cm; k = 1, LASTCV
NA1		Charge and mass of a disk change from first value to second value at end of $NA1^{th}$ cavity (NA1 needs to be loaded only if NUMA > 1.)
NA2		Charge and mass of a disk change from second value to third value at end of $NA2^{th}$ cavity (NA2 needs to be loaded only if NUMA = 3.)
NB1		Beam radius changes from first value to second value at end of $NB1^{th}$ cavity (NB1 needs to be loaded only if NUMB > 1.)
NB2		Beam radius changes from second value to third value at end of $NB2^{th}$ cavity (NB2 needs to be loaded only if NUMB = 3.)
NBWM		Number of last cavity considered in calculating backward wave
NCAVSS		Number of cavity for which small-signal parameters are calculated
NDISKS	N_d	Number of disks (NDISKS ≤ 48)

Name	Symbol	Description
NMAX		For sums that are stored in tables, excluding space charge force tables, NMAX is the upper limit (NMAX $\leq$ 40)
NUMA		Number of discrete values for the charge and mass of a disk (1 $\leq$ NUMA $\leq$ 3)
NUMB		Number of discrete values for the beam diameter (1 $\leq$ NUMB $\leq$ 3)
NVEL		Number of cavities for which disk velocities are to be printed out (See KVEL for related input.)
NXGRID	N_z	Number of nodes per cavity. NXGRID must be divisible by 4 (8 $\leq$ NXGRID $\leq$ 64).
NXISC		Number of data points in each space charge force table (NXISC $\leq$ 200)
PINDBM		Input power, dBm
SCMAX		If the maximum separation between two disks is greater than SCMAX disk lengths, the space charge force on one disk due to the other is set to zero. SCMAX should equal an integer plus one-half.
TOLDV		Error criterion for determining whether an additional pass through a cavity is required. If $\left\| \frac{\Delta V_{f,new} - \Delta V_{f,old}}{V_{f,new}} \right\| > \text{TOLDV}$ then an additional pass is made.
TOLSC		Error criterion for determining whether the frequency of calculating space charge forces should be doubled. If for any disk the difference between the calculated space charge force and the extrapolation of the quadratic curve fit is greater than the product of TOLSC and the maximum rf electric field force

Name	Symbol	Description
		in the cavity, the frequency of calculating space charge forces is doubled.
V0B	V_0	Beam voltage, V
VJUMP(K)	V_{Jk}	The dc voltage jump for k^{th} cavity, V; k = 1, LASTCV
ZIMP(K)	Z_k	If KIMP = 0, ZIMP(K) is the Pierce impedance in ohms for k^{th} cavity; k = 1, LASTCV. If ZIMP = 1, ZIMP(K) is the total impedance in ohms for k^{th} cavity; k = 1, LASTCV.

DESCRIPTION OF OUTPUT DATA

The program output consists of both printed output and plots. The plots are produced only if the input parameter KPLOT is zero. The printed output includes three parts: (1) printing of small-signal parameters (only if the input parameter KSMSIG is zero); (2) a cavity-by-cavity printing of selected data; (3) printing of normalized disk velocities at selected cavities. The program can be easily modified to calculate and print other data if desired. The format of the output can be seen in the sample problem of appendix B.

First, the input data are printed in NAMELIST format. (The printing of the input data can be suppressed by letting KPRINT be nonzero.) Then the small-signal parameters are printed if desired. The small-signal parameters are as follows:

Name	Symbol	Description
U0	u_0	Initial beam velocity, m/sec
BEB	$\beta_e b$	Product of beam propagation constant and beam radius
B1B	$\beta_1 b$	Product of wave propagation constant and beam radius
KP	K_p	Pierce impedance, ohms
ZC	Z_c	Total impedance, ohms

Name	Symbol	Description
C	C	Pierce's C
B	b	Pierce's b
D	d	Pierce loss parameter d
DGAIN		Asymptotic gain per cavity, dB/cavity
QQ	Q	Pierce's space charge parameter, QC/C
A1PA2	$A_1 + A_2$	Launching loss, dB

The following data are printed for each cavity:

Name	Description
CAV	Cavity number
VMAG	Magnitude of gap voltage, V
VPHA	Phase of gap voltage divided by π
ISMAG	Magnitude of normalized induced current
ISPHA	Phase of normalized induced current divided by π
VPHA-ISPHA	VPHA minus ISPHA
LS GAIN	Large-signal gain, dB
POUT	Output power, W
EFF	Efficiency
PKE	Change in beam kinetic power referred to initial beam kinetic power, W
PFW	Power in forward wave, W
PBW	Power in backward wave, W
PLC	Cumulative power loss, W

Name	Description
PBAL	Power balance equal to $$1 + \frac{PKE - PJUMP + PFW + PBW + PLC}{I_0 V_0}$$ where PJUMP is the power due to all voltage jumps up to the current cavity
ITER	Number of iterations of the beam disks traversing the cavity
SC	Space charge forces are calculated every SC steps.

Figure 4 is an example of the plotted output. The figure is a form of Applegate diagram. We calculate φ_{ki}, the phase of the forward voltage seen by the i^{th} disk when it is at the middle of the gap in the k^{th} cavity, as

$$\varphi_{ki} = \tan^{-1}\left\{\frac{\mathcal{Im}\left[V_{fk}\, e^{i\omega t_i(z_{k,mid})}\right]}{\mathcal{Re}\left[V_{fk}\, e^{i\omega t_i(z_{k,mid})}\right]}\right\}$$

The parameter φ_{ki} is plotted as a function of k. There are $\frac{1}{2} N_d$ plots, one for every other disk.

DESCRIPTION OF GLOBAL VARIABLES

Global variables are variables that are used by more than one subroutine and hence are put into COMMON blocks. In the following descriptions, we exclude input data variables since these have already been described.

Name	Symbol	Description
A	a	Tunnel radius, m
ALPHLB(K)	$(\alpha L)_{bk}$	Voltage attenuation of backward wave in going from cavity $k + 1$ to cavity k, dB per cavity; $k = 1$, LASTCV

Name	Symbol	Description
B(I)	b	I^{th} beam radius, m; I = 1, NUMB
C	c	Speed of light
C1(I)		Constant associated with I^{th} beam diameter; I = 1, NUMB
C2(I)		Constant associated with I^{th} beam diameter; I = 1, NUMB
C3		Constant associated with calculation of forces due to voltage jumps
CNORM	$\frac{c}{\omega a}$	Normalized speed of light
COSY(I)		Array of cosine values used in subroutine TABLE; I = 1, 2*NXGRID + 1
CTHETA	$\cos\theta$	Cosine of normalized time
CURRNT		Fundamental Fourier component of current
DELV(K)	ΔV_{fk}	Forward induced voltage for k^{th} cavity, V; k = 1, LASTCV
DELVR(K)	ΔV_{bk}	Backward induced voltage for k^{th} cavity, V; k = 1, LASTCV
DELX(I)	$\Delta\xi$	Integration step size in I^{th} cavity string; I = 1, NSCAV
DELXSC		Spacing between points in space charge force tables
DPR		Degrees per radian, DPR = $180/\pi$
DVRTEM(K)	ΔV_{bk}	Backward induced voltage of previous case, for k^{th} cavity, V; k = 1, LASTCV
DVTEMP(K)	ΔV_{fk}	Approximate forward induced voltage for k^{th} cavity, obtained by assuming disks have constant velocity throughout cavity, V; k = 1, LASTCV

Name	Symbol	Description
ECHARG	e	Charge of an electron (ECHARG is positive.)
EMASS	m_e	Mass of an electron
EPS0	ϵ_0	Permittivity of free space
FORIER(K)		Fourier coefficient of fundamental harmonic of induced current in k^{th} cavity; $k = 1$, LASTCV
FREQ	f	Frequency, Hz
I0B	I_0	Beam current at tube entrance, A
ISCAV(K)		Number of cavity string in which k^{th} cavity is located; $k = 1$, LASTCV
ITER		Present number of iteration of beam disks traversing cavity
ITERSV		Total number of iterations of beam disks traversing cavity
KBEGIN		Equals zero at beginning of a case and is set equal to 1 immediately thereafter
KCAV		Number of current cavity
KOUNTP		Counts points to be plotted
KPDZC(K)		Ratio of Pierce impedance to total impedance for k^{th} cavity; $k = 1$, LASTCV
KSCAV		Number of present cavity string (A cavity string is a string of consecutive cavities all having the same geometrical and electrical properties.)
KSCF		Space charge forces are calculated every KSCF steps
KSTOP		Equals zero until end of last cavity, when it is set equal to 1
KX		Number of current node, counted from first node of first cavity

Name	Symbol	Description
KX0		Initial node of present case, counted from first node of first cavity
KXPRI		Number of current node, counted from first node of current cavity
KXSC		Number of node, counted from first node of first cavity, at which the most recent calculation of space charge forces was done
LAMB	λ	Beam wavelength, m
LCIR(K)	L_k	Length of K^{th} cavity, m; k = 1, LASTCV
LDISK	l_d	Axial length of a disk, m
LDISKN	l_d/a	Normalized axial length of a disk
LSMALL(K)	l_k	One-half of gap length in k^{th} cavity, m; k = 1, LASTCV
MDISK(I)	m_d	Mass of a disk in I^{th} interception region, kg; I = 1, NUMA
MUA(I)	λ_i	I^{th} zero of Bessel function J_0; I = 1, 40
NB		Number of current beam-diameter region (A beam-diameter region is a region throughout which the beam diameter is constant.)
NCASE		Number of current case
NCAVPS(I)		Number of cavities in I^{th} cavity string; I = 1, NSCAV
NCUMCS(I)		Number of last cavity in I^{th} cavity string; I = 1, NSCAV
NQ		Number of present interception region
NSCAV		Total number of cavity strings
P0B		Linear current density, C/m

Name	Symbol	Description
PBW(K)		Power in backward wave in k^{th} cavity, W; k = 1, LASTCV
PFW(K)		Power in forward wave in k^{th} cavity, W; k = 1, LASTCV
PI	π	PI = 3.1415927
PJUMP(K)		Power due to all voltage jumps up to k^{th} cavity, W; k = 1, LASTCV
PKE(K)		Kinetic power at end of k^{th} cavity minus kinetic power at beginning of tube, W; k = 1, LASTCV
PLC(K)		Cumulative power loss at end of k^{th} cavity, W; k = 1, LASTCV
POBAL		Power balance
QDISK(I)		Charge of a disk in I^{th} interception region, C; I = 1, NUMA
SBET0A(I)	$\beta_0 a$	Value of $\beta_0 a$ for cavities in I^{th} cavity string; I = 1, NSCAV
SCA1(I)		I^{th} entry in table of space charge forces for first beam diameter; I = 1, NXISC+1
SCA2(I)		I^{th} entry in table of space charge forces for second beam diameter; I = 1, NXISC+1
SCA3(I)		I^{th} entry in table of space charge forces for third beam diameter; I = 1, NXISC+1
SIMPS(I)	δ_i	I^{th} coefficient for Simpson's rule integration; I = 1, NXGRID
SINY(I)		Array of sine values used in subroutine TABLE; I = 1, 2*NXGRID+1
SLCIR(I)		Length of cavities in I^{th} cavity string, m; I = 1, NSCAV

Name	Symbol	Description
SLSMAL(I)		One-half of gap length for cavities in I^{th} cavity string, m; I = 1, NSCAV
SR1MB2		SR1MB2 = $\sqrt{1 - (u_0/c)^2}$
SSGAIN(K)		Small-signal gain at k^{th} cavity, based on small-signal calculations using geometrical and electrical properties of cavity number NCAVSS; k = 1, LASTCV
STHETA	$\sin \theta$	Sine of normalized time
THT(I)	θ_i	Value of normalized time of arrival of I^{th} disk at current axial position ξ; I = 1, NDISKS
THTP(I)	$\frac{d\theta_i}{d\xi}$	First derivative with respect to ξ of θ_i; I = 1, NDISKS
THTPP(I)	$\frac{d^2\theta_i}{d\xi^2}$	Second derivative with respect to ξ of θ_i; I = 1, NDISKS
TWOPI	2π	TWOPI = 6.2831853
TXR(I, 1)		Real part of I^{th} entry in table needed to calculate induced voltages; I = 1, NXGRID
TXI(I, 1)		Imaginary part of I^{th} entry in table needed to calculate induced voltages; I = 1, NXGRID
TXR(I, 2)		Real part of I^{th} entry in table needed to calculate rf electric field forces; I = 1, NXGRID
TXI(I, 2)		Imaginary part of I^{th} entry in table needed to calculate rf electric field forces; I = 1, NXGRID
TXR(I, 3)		I^{th} entry in table needed to calculate voltage-jump forces; I = 1, NXGRID
U0B		Initial beam velocity, m/sec

Name	Symbol	Description
U0NORM	$\frac{u_0}{\omega a}$	Normalized initial beam velocity
V0BSUM(K)		Beam voltage plus sum of all voltage jumps up to k^{th} cavity, V; k = 1, LASTCV
VGAP(K)	V_k	Sum of forward voltage and backward voltage for k^{th} cavity, V; k = 1, LASTCV
VGAPF(K)	V_{fk}	Forward voltage for k^{th} cavity, V; k = 1, LASTCV
VGAPR(K)	V_{bk}	Backward voltage for k^{th} cavity, V; k = 1, LASTCV
VGAP1M		Voltage across first gap, V
W	ω	Radian frequency, rad/sec
X	ξ	Current value of normalized position along tube axis, measured from beginning of first cavity
X0	ξ_0	Initial value of normalized position along tube axis for the present case, measured from beginning of first cavity
XICAV(K)		Normalized axial position at end of k^{th} cavity; k = 1, LASTCV
XIMXSC		Maximum normalized separation distance in space charge force tables (If two disks are separated by a distance greater than XIMXSC, the space charge force on one disk due to the other is set to zero.)
XISC1		One of three latest values of ξ at which space charge forces were calculated
XISC2		One of three latest values of ξ at which space charge forces were calculated
XISC3		One of three latest values of ξ at which space charge forces were calculated

Name	Symbol	Description
XISCAV(I)		Normalized axial position at end of I^{th} cavity string; I = 1, NSCAV
XPRI		Present value of normalized position along tube axis, measured from beginning of current cavity
XSCA(I)		Coefficient in quadratic curve fit of space charge force on I^{th} disk; I = 1, NDISKS
XSCB(I)		Coefficient in quadratic curve fit of space charge force on I^{th} disk; I = 1, NDISKS
XSCC(I)		Coefficient in quadratic curve fit of space charge force on I^{th} disk; I = 1, NDISKS
XSC1(I)		Third most recent evaluation of space charge force on I^{th} disk; I = 1, NDISKS
XSC2(I)		Second most recent evaluation of space charge force on I^{th} disk; I = 1, NDISKS
XSC3(I)		Most recent evaluation of space charge force on I^{th} disk; I = 1, NDISKS
ZC(K)		Total impedance for k^{th} cavity, ohms, k = 1, LASTCV

DESCRIPTION OF SUBROUTINES

In this section, the COMMON blocks, the main program, and each subroutine are described. Flow charts are included for the more complex subroutines.

COMMON Blocks

The program has five COMMON blocks. COMMON/INDATA/ contains the input data. COMMON/MREAL/ contains real and integer global variables. COMMON/MCOMP/ contains complex global variables. COMMON/PLOT/ contains arrays used for plotting Applegate diagrams. COMMON/STATE/ contains arrays used for storing

initial states and final states. An initial state is a collection of variables whose values are those at the beginning of the first cavity in the tube section under consideration. A final state is the same collection of variables but whose values are those at the end of the last cavity in the tube section. The variables in this collection are those whose values must be known in order to start the simulation of a tube section. It is necessary to store these initial and final states because they may be used in later cases. For example, in simulating the second tube section, we use the final state of the first tube section as a startup.

Main Program

The main program reads the first 40 zeros of the Bessel function J_0. Subroutines STDAT, INDAT, and SMSIG are then called. When the last integration step has been done, the final state is stored in COMMON/STATE/. Depending on the value of ISTATE, the final state may also be stored in a data set for possible use in a future case. The main program calls XINT to integrate one step and calls BTWNS to check on what action should be taken between steps.

Subroutine ACC

Subroutine ACC is called by subroutine XINT. Subroutine ACC calculates the normalized acceleration, ACCX, of each disk. The accelerations result from three forces: space charge force, rf electric field force, and voltage-jump force. The accelerations due to space charge forces are obtained by quadratic curve fits, and the accelerations due to rf electric field force and voltage-jump force are calculated in subroutine RFACC. Subroutine ACC also calculates THTPP(I), the second derivative of the function $\theta_i(\xi)$.

The local variables are defined as follows:

ACCX	Normalized acceleration of a disk
EXACC	Normalized acceleration of a disk due to rf electric field force and voltage-jump force
KXPRI	Integer indicating location of table values for current value of ξ
RELCOR	Relativistic correction factor
SXACC	Normalized acceleration of a disk due to space charge forces

XPRI Current value of ξ measured from beginning of current cavity

XREL Current value of ξ measured from the last value of ξ for which space charge forces were calculated

Subroutine APPLE

Subroutine APPLE is called by the main program. Subroutine APPLE manipulates plot data and calls plot routines for plotting Applegate diagrams.

The local variables are defined as follows:

BREAK Logical variable; true if two successive data points are more than 180° apart (indicates these two points should not be joined on plots by straight line segment)

KEND Logical variable; true if the current data point is the last data point

NCURVS Number of curves (NCURVS = $\frac{1}{2} N_d$)

NPTS Number of points per curve

XDOWN X array of points to be plotted

YACROS Y array of points to be plotted

Subroutine BTWNC

A flow chart of subroutine BTWNC is given in figure 5. Subroutine BTWNC is called by subroutine BTWNS when the end of a cavity is reached. Subroutine BTWNC determines whether another pass through the cavity is required. A second pass is not required if either of two conditions is met: (1) a second pass has already been made, or (2) the induced forward voltage is sufficiently close to the approximation of the induced forward voltage obtained by assuming constant disk velocities throughout the cavity.

If a second pass is not required, the subroutine sets up for entrance into the new cavity. If needed, new tables are calculated by calling subroutine TABLE. Since a second pass through the new cavity may be needed, it is necessary to store the state at the beginning of the new cavity. Subroutine FSAPP is called to calculate DVTEMP, the approximation to the induced forward voltage for the new cavity. The new forward voltage is then calculated by phase shifting and attenuating the old forward voltage and adding

DVTEMP. If plots are desired, an approximation to the forward voltage for the cavity following the new cavity is required. We calculate this voltage in the same manner that we calculated the forward voltage for the new cavity.

The local variables are defined as follows:

KSWICH Determines which way to branch after calculating VGAP(KCAV)

H or HOLD Appending H or HOLD to a variable name indicates that the variable is being held in temporary storage in case it is needed again when a second pass through a cavity is made.

T or TEMP Appending T or TEMP to a variable name indicates that the variable is being held in temporary storage.

Subroutine BTWNS

Subroutine BTWNS is called by MAIN. Subroutine BTWNS determines what action should be taken between integration steps. First, the subroutine determines whether a new space charge calculation is required. A new calculation is required if the last calculation was KSCF steps ago or if the current value of ξ is at a boundary between two beam-diameter regions. Next, the subroutine determines whether the end of a cavity has been reached. If so, subroutine BTWNC is called. Finally, the subroutine determines whether subroutine PLOTS should be called. Except in the first and last cavities, subroutine PLOTS is called four times per cavity.

The local variables are defined as follows:

LSCFIT Logical variable; true if current value of ξ is at a boundary between two beam-diameter regions

NN(1) Beam diameter changes from first value to second value at end of cavity NN(1)

NN(2) Beam diameter changes from second value to third value at end of cavity NN(2)

Subroutine CAVP

Subroutine CAVP is called by surboutine INDAT. Subroutine CAVP calculates quantities related to cavities and cavity strings. A cavity string is a string of con-

secutive cavities all having the same electrical and geometrical properties. The number of cavities cannot exceed 650, and the number of cavity strings cannot exceed 35.

Subroutine CKPDZ

Subroutine CKPDZ is called by surroutine INDAT. Subroutine CKPDZ calculates KPDZC(K), the ratio of Pierce impedance to total impedance, for the k^{th} cavity.

Subroutine CROOT

Subroutine CROOT is called by subroutine SMSIG. Subroutine CROOT calculates the roots of the quartic polynomial involved in calculating small-signal parameters. The subroutine first solves for the roots of the cubic polynomial using the Newton-Raphson method. Using these roots as the first iterates, the subroutine then uses the Newton-Raphson method to solve for the roots of the quartic polynomial.

Subroutine DVSUM

Subroutine DVSUM is called by subroutine XINT. Subroutine DVSUM calculates one term in the summation for the induced forward voltage, DELV, and one term in the summation for the induced backward voltage, DELVR. These terms are added to the running sums for DELV and DELVR. The summations are those given in equations (33) and (34).

Subroutine ENBAL

Subroutine ENBAL is called by subroutine BTWNC. Subroutine ENBAL calculates the power balance at the end of the cavity in question. There are five terms in the power balance: PKE, PJUMP, PFW, PBW, and PLC. PKE is the kinetic power minus the initial kinetic power. PJUMP is the power due to all voltage jumps up to the cavity in question. PFW is the power in the forward wave minus the power in the forward wave in the first cavity. PBW is the power in the backward wave. PLC is the sum of power losses up to the present cavity. Power balance is equal to one plus the sum of these five terms divided by the initial beam power.

The local variables are defined as follows:

ATTENF	Attenuation factor for forward wave
ATTENR	Attenuation factor for backward wave
ICL	Number of the cavity in question
I0BV0B	Product of beam current and beam voltage
PBIP2	Power in backward wave in cavity ICL + 2
PF1	Power in forward wave in first cavity
PFI	Power in forward wave in cavity ICL
PFIM1	Power in forward wave in cavity ICI - 1

Subroutine FSAPP

Subroutine FSAPP is called by subroutine BTWNC. Subroutine FSAPP calculates an approximation, DVTEMP, to the induced forward voltage by assuming the disks have constant velocity in the cavity under consideration.

Subroutine INDAT

Subroutine INDAT is called by the main program. The subroutine first reads input data from a prestored data set. It then reads data entered at the terminal in NAMELIST format. Only input data that differ from those in the prestored data set need to be entered. The input data are stored in a data set for possible future use. The subroutine then calculates constants and initializes variables. The initial state is obtained in one of three ways: (1) if the input parameter ISTATE is 4, the initial state is read from a data set; (2) if ISTATE is not 4 and INITCV (initial cavity) is 1, the initial state is calculated from input data; (3) if ISTATE is not 4 and INITCV is not 1, the initial state is obtained from COMMON/STATE/. There is storage allotment for three states in COMMON/STATE/. Which of the three is chosen is determined by ISTATE (see definition of ISTATE in the section on description of input data).

After the initial state is obtained, it is stored in COMMON/STATE/ in the first of the three storage allotments. This is done because the initial state of the present case may be used as the initial state in the following case. and thus it must be stored. The

initial state is also stored in the third of the three storage allotments if the input parameter ISAVE is an odd integer. This is done because the initial state of the present case may also be required as the initial state in some future case after the following case, and thus it must be stored.

The input parameter ISAVE is the sum of I1, I2, and I3 (see definition of ISAVE in the section on description of input data). If I2 is 2, the initial state of the present case is stored in a specified data set for possible use in a future case.

If INITCV is 1, subroutine INDAT calculates the forward voltage for the first cavity. If INITCV is not 1, the forward voltage for the cavity previous to cavity INITCV is required for startup. This voltage will be known either from the previous case or by reading it from a data set. The backward voltages are calculated next. Finally, the induced backward voltages DELVR are stored in the array DVRTEM. This is done because in the equations of motion we must use the induced backward voltages of the previous case. We cannot use the DELVR array because this array changes during the simulation as the new induced backward voltages are calculated. We therefore use the DVRTEM array in the equations of motion.

Subroutine NATTN

Subroutine NATTN is called by subroutines BTWNC and SCFIT. Subroutine NATTN calculates the number of the interception region in which XXX is located.

Subroutine NR

Subroutine NR is called by subroutines BTWNC and SCFIT. Subroutine NR calculates the number of the beam-diameter region in which XXX is located.

Subroutine OUTPT

Subroutine OUTPT is called by subroutine BTWNC. Subroutine OUTPT calculates and prints output data. Since the output data have already been described in another section, we will not repeat the description here.

Subroutine PLOTS

Subroutine PLOTS is called four times per cavity by subroutine BTWNS. For every other disk i, subroutine PLOTS calculates φ_{ki}, the phase of the forward voltage seen by the i^{th} disk when it is at the middle of the gap in the k^{th} cavity. Although there is only one φ_{ki} per cavity per disk, it is desirable to plot more points per cavity per disk to obtain smoother plots. An interpolation procedure is used to obtain four points per cavity per disk. When ξ is in the first half of the cavity, the subroutine calculates a voltage VV by interpolating between voltages in the previous cavity and the present cavity. When ξ is in the second half of the cavity, the subroutine calculates VV by interpolating between voltages in the present and following cavities. The phase angle φ_{ki} is then calculated as the phase of VV.

The local variables are defined as follows:

PHIK	Phase angle φ_{ki}
SHALF	Logical variable; true if ξ is located in second half of current cavity or if current cavity is cavity INITCV
T1	Normalized time at which disk is at center of previous gap
T2	Normalized time at which disk is at center of present gap
T3	Normalized time at which disk is at center of following gap
V1	Forward voltage, in previous cavity, whose phase is that seen by disk when it is at center of gap
V2	Forward voltage, in present cavity, whose phase is that seen by disk when it is at center of gap
V3	Forward voltage, in following cavity, whose phase is that seen by disk when it is at center of gap
VV	Interpolated value of forward voltage
X1	Normalized axial position at center of previous gap
X2	Normalized axial position at center of present gap
X3	Normalized axial position at center of following gap

Subroutine RFACC

Subroutine RFACC is called by subroutine ACC. Subroutine RFACC calculates EXACC, the normalized acceleration of a disk due to rf electric field force and voltage-jump force.

The local variables are defined as follows:

EXACC	Normalized acceleration of a disk due to rf electric field force and voltage-jump force
VF	Forward voltage at time disk arrives at current value of ξ
VR	Backward voltage at time disk arrives at current value of ξ

Subroutine SCACC

Subroutine SCACC is called by subroutine SCFIT. Subroutine SCACC calculates the space charge acceleration of one disk due to another by linear interpolation on space charge force tables. Although we use the term space charge force tables, these tables actually evaluate accelerations rather than forces. If the two disks are in two different beam-diameter regions, two linear interpolations are done and the average is taken.

The local variables are defined as follows:

NREF	Number of beam-diameter region of reference disk
NSRC	Number of beam-diameter region of source disk
SCA0	Space charge acceleration of reference disk

Subroutine SCAT

Subroutine SCAT is called by subroutine INDAT. For each beam diameter IB and for the I^{th} separation distance X, subroutine SCAT calculates the space charge acceleration SCATMP (I, IB) of one disk due to another. Using EQUIVALENCE statements, we put SCA1, SCA2, and SCA3 into COMMON/MREAL/ instead of SCATMP. The arrays SCA1, SCA2, and SCA3 make up the space charge force tables. In this subroutine, X is used as the separation distance between disks. Since X is also used as a global variable (current value of ξ), it is necessary to save the global variable in XSAVE. At the end of the subroutine, the value of the global variable is returned to X.

Subroutine SCAT also calculates ZRATIO, the ratio of the largest space charge acceleration to the smallest. The smallest space charge acceleration occurs when the separation distance is largest. The largest separation distance is determined by the input variable SCMAX.

The local variables are defined as follows:

LDISKR	Relativistic thickness of a disk, m
SCAMAX	Maximum space charge acceleration of one disk due to another disk
SCATMP (I, IB)	For the IBth beam diameter and the Ith separation distance, the space charge acceleration of one disk due to another
X	Separation distance between disks
XSAVE	Temporary storage for global variable X
ZMAX	For the largest separation distance, ZMAX is the largest space charge acceleration among the beam diameters
ZRATIO	The ratio of the largest space charge acceleration to the smallest

Subroutine SCFIT

Subroutine SCFIT is called by subroutine BTWNS. Subroutine SCFIT first calculates what the space charge accelerations would be if the present curve fits are used. Then for each disk the subroutine calculates the space charge acceleration of the disk by summing the accelerations due to all the other disks. The acceleration of one disk due to another is obtained by linear interpolation on the space charge force tables. The coefficients of the new quadratic curve fits are then calculated. Finally, the subroutine determines whether the frequency of the space charge calculation should be changed. This is done by comparing the space charge accelerations based on the old curve fits with those just calculated. If the difference for any disk is greater than the product of TOLSC and the maximum acceleration due to the rf electric field in the cavity, the frequency of calculating space charge accelerations is doubled.

The local variables are defined as follows:

ARG	Normalized separation distance between reference disk and source disk
ERRSC(I)	For the ith disk, the difference between the space charge acceleration based on the old curve fits and the space charge accelerations just calculated

NBSRC Number of beam-diameter region of source disk

NREF Number of beam-diameter region of reference disk

SCAMAX Maximum value in array ERRSC

SXACC(I) For i^{th} disk, the space charge acceleration based on the old curve fits

THTREF Current value of θ for reference disk

XREL Current value of ξ relative to last value of ξ for which space charge forces were calculated

Subroutine SMSIG

Subroutine SMSIG is called by the main program. Subroutine SMSIG calculates small-signal parameters as given in reference 8. The Pierce C parameter is given by

$$C = \left(\frac{K_p I_0}{4V_0}\right)^{1/3}$$

where K_p is the Pierce impedance. The Pierce velocity parameter is given by

$$b = \frac{u_0 - \frac{\omega}{\beta_1}}{\frac{\omega C}{\beta_1}}$$

The Pierce loss parameter is given by

$$d = \frac{\frac{\alpha L}{20} \log_{10} e}{\frac{\omega L C}{u_0}}$$

The plasma frequency ω_q is given by

$$\omega_q = \sqrt{\frac{R^2 N e^2}{m_e \epsilon_0}}$$

where R is the plasma frequency reduction factor obtained by table lookup and N is

$$N = \frac{q_d}{e \, l_d \pi b^2}$$

The Pierce Q parameter is given by

$$Q = \frac{\omega_q^2}{4C^3 (\omega + \omega_q)^2}$$

The roots δ_1, δ_2, and δ_3 are those of the cubic equation

$$\delta^2 = \frac{1}{-b + jd + j\delta} - 4QC$$

The roots of the cubic equation are only approximate. The exact roots are those of the quartic equation

$$\delta^2 = \frac{(1 + Cb - jCd)(1 + Cb)^2}{-b + jd + j\delta - \frac{C}{2}\left[\delta^2 + (b - jd)^2\right]} - 4QC$$

The launching loss is given by

$$A_1 + A_2 = 20 \log \left| \frac{\delta_1^2 + 4QC}{(\delta_1 - \delta_2)(\delta_1 - \delta_3)} \right|$$

The gain per cavity in dB is given by

$$\Delta G = \frac{54.6 \, \mathcal{R}e \, (\delta_1) CL}{\lambda}$$

where λ is the beam wavelength and L is the length of the cavity.

The local variables are defined as follows:

A1PA2	Launching loss, A1 + A2
BB	Pierce velocity parameter b
CC	Pierce parameter C
DDD	Pierce loss parameter d
DEL(I)	I^{th} root of quartic polynomial
DGAIN	Gain per cavity, dB per cavity
KP	Pierce impedance, ohms
QQ	Pierce parameter Q
R	Plasma frequency reduction factor
SSGAIN(K)	Small-signal gain at k^{th} cavity, dB
WQ	Plasma frequency, rad/sec

Subroutine STDAT

Subroutine STDAT is called by the main program. Subroutine STDAT calculates standard data, that is, constants whose values are independent of input data.

Subroutine TABLE

A flow chart for subroutine TABLE is given in figure 6. Subroutine TABLE is called by subroutine BTWNC when a new cavity is entered and tables have to be computed for the new cavity. If the new cavity has the same properties as the old cavity, subroutine TABLE is not called. The subroutine calculates the following tables:

TXR(n, 1), TXI(n, 1)	Real and imaginary parts of the table S_{nk} needed to calculate induced voltages; n = 1, . . ., NXGRID

TXR(n, 2), TXI(n, 2) Real and imaginary parts of the table Q_{nk} needed to calculate rf electric field forces; n = 1, ..., NXGRID

TXR(n, 3) Table R_{nk} needed to calculate voltage-jump forces; n = 1, ..., NXGRID

From equation (32), dropping the subscript k, we obtain

$$\mathrm{TXR}(n,1) + i\,\mathrm{TXI}(n,1) \equiv S_n^* = \sum_{m=-\infty}^{\infty} P_m e^{-i\left(\beta_0+\frac{2\pi m}{L}\right)y_n} \tag{39}$$

From equation (21), dropping the subscript k, we can define W_m such that

$$\mathrm{TXR}(n,2) + i\,\mathrm{TXI}(n,2) \equiv Q_n = \sum_{m=-\infty}^{\infty} W_m e^{-i\left(\beta_0+\frac{2\pi m}{L}\right)y_n} \tag{40}$$

From equations (23) to (25), dropping the subscript k, we can define T_m, U_m, and Y_m such that

$$\mathrm{TXR}(n,3) \equiv R_n = T_0 + \sum_{m=1}^{\infty} T_m \cos\left(\frac{2m\pi y_n}{L}\right) \tag{41}$$

or

$$\mathrm{TXR}(n,3) \equiv R_n = U_0 + \sum_{m=1}^{\infty} U_m \cos\left(\frac{2m\pi|y_n|}{L}\right) + Y_m \sin\left(\frac{2m\pi|y_n|}{L}\right) \tag{42}$$

Equations (39) and (40) can be rewritten as

$$\mathrm{TXR}(n,1) + i\,\mathrm{TXI}(n,1) = e^{-i\beta_0 y_n} \sum_{m=-\infty}^{\infty} P_m e^{-i\left(\frac{2\pi m y_n}{L}\right)} \tag{43}$$

$$\mathrm{TXR}(n,2) + i\,\mathrm{TXI}(n,2) = e^{-i\beta_0 y_n} \sum_{m=-\infty}^{\infty} W_m e^{-i\left(\frac{2\pi m y_n}{L}\right)} \tag{44}$$

From equations (41) to (44), it is clear that a significant amount of the computer time for calculating tables is spent on evaluating $\cos(2\pi m y_n/L)$ and $\sin(2\pi m y_n/L)$. Subroutine TABLE uses a scheme that significantly reduces the computer time for evaluating these trigonometric functions. For given values of m and n, we define k_1 and k_2 such that

$$\left(m - \frac{N_z}{2}\right)(2n - 1) = k_1(2N_z) + k_2 \qquad 0 \le k_2 \le 2N_z - 1$$

Then it can be shown that

$$\cos\left(\frac{2\pi m y_n}{L}\right) = \cos\left(\frac{2\pi k_2}{2N_z}\right) \qquad 0 \le k_2 \le 2N_z - 1$$

$$\sin\left(\frac{2\pi m y_n}{L}\right) = \sin\left(\frac{2\pi k_2}{2N_2}\right) \qquad 0 \le k_2 \le 2N_z - 1$$

Thus, the trigonometric functions take on only $2N_z$ distinct values. These values are calculated once in subroutine INDAT and stored in the arrays COSY and SINY. Subroutine TABLE needs only to calculate k_2 to obtain the trigonometric functions.

Subroutine TABLE calculates the tables for positive values of y_n (right half of cavity). Symmetry is then used to obtain the tables for negative values of y_n (left half of cavity).

The local variables are defined as follows:

COSB0Y(N)	$\cos(\beta_0 z_{nk})$, where k is the number of the cavity in question
COSDEL	$\cos(\beta_0 L_k/N_z)$, where k is the number of the cavity in question
FAC(1, NN)	Array used in calculating TXR(IZ, 1) and TXI(IZ, 1)
FAC(2, NN)	Array used in calculating TXR(IZ, 2) and TXI(IZ, 2)
FAC(3, NN)	Array used in calculating TXR(IZ, 3)
FAC(4, NN)	Array used in calculating TXR(IZ, 3)
FAC(5, NN)	Array used in calculating TXR(IZ, 3)
LJUMP	Equals zero if TXR(IZ, 3) is to be calculated; equals 1 otherwise
NMAXP1	NMAX+1
NNMAX	2*NMAX+1
NXDUBL	2*NXGRID
NXHALF	NXGRID/2
SINB0Y(N)	$\sin(\beta_0 z_{nk})$, where k is the number of the cavity in question
SINDEL	$\sin(\beta_0 L_k/N_z)$, where k is the number of the cavity in question
Y	Axial position relative to center of gap

Subroutine XINT

Subroutine XINT is called by the main program. Subroutine XINT integrates the equations of motion over one step. The numerical integration method is described in the section on the dynamics of beam disks.

CONCLUDING REMARKS

The use of the coupled-cavity traveling wave tube for space communications had led to an increased interest in improving the efficiency of the basic interaction process in

these devices through velocity resynchronization and other methods. In order to analyze these methods, we have recently developed a flexible large-signal computer program for use on the IBM 360/67 time-sharing system. The present report is a users' manual for this program. The report describes the program in sufficient detail to allow a user to make modifications in the program if desired.

Lewis Research Center,
National Aeronautics and Space Administration,
Cleveland, Ohio, May 5, 1977,
506-20.

APPENDIX A

SYMBOLS

a	tunnel radius
b	beam radius
C_{mk}	factor used in tables, defined in eq. (17)
c	speed of light
e	charge of electron
F_{zi}	axial force on i^{th} disk
f	frequency
I_0	beam current at tube entrance
$J_1(z)$	fundamental Fourier component of current density at z
L_k	length of k^{th} cavity
l_d	axial thickness of a disk
l_k	half-length of k^{th} gap
m_d	mass of a disk
m_e	mass of an electron
N_b	number of beam-diameter regions
N_c	number of cavities
N_d	number of disks per beam wavelength
N_z	number of nodes per cavity
P_k	power, k^{th} cavity
Q_{nk}	table for calculation of rf forces
q_d	charge of a disk
R_{nk}	table for calculation of voltage-jump forces
S_{nk}	table for calculation of induced voltages
T	reciprocal of frequency
$t_i(z)$	time of arrival of i^{th} disk at axial location z
u_0	initial beam velocity

V_{bk}	backward voltage, k^{th} cavity
V_{fk}	forward voltage, k^{th} cavity
ΔV_{bk}	backward induced voltage, k^{th} cavity
ΔV_{fk}	forward induced voltage, k^{th} cavity
V_0	beam voltage
V_{Jk}	voltage jump, k^{th} cavity
V_k	gap voltage, k^{th} cavity
$v_i(z)$	velocity of i^{th} disk at axial location z
y_{nk}	axial position, relative to center of k^{th} cavity, of n^{th} node in cavity
Z_k	interaction impedance for k^{th} cavity
z_{nk}	axial position, relative to beginning of first cavity, of n^{th} node in k^{th} cavity
Δz_k	integration step size in k^{th} cavity
$(\alpha L)_{bk}$	loss factor for backward voltage in k^{th} cavity
$(\alpha L)_{fk}$	loss factor for forward voltage in k^{th} cavity
β_{mk}	propagation factor, defined in eq. (18)
$(\beta_1 L)_k$	phase shift of voltage for k^{th} cavity
γ_{mk}	factor used in tables, defined in eq. (19)
δ_n	n^{th} coefficient for Simpson's rule integration
ϵ_0	permittivity of free space
$\theta_i(\xi)$	normalized time of arrival of i^{th} disk at normalized axial location ξ
λ	wavelength
μ	shaping parameter for electric field
ξ	normalized axial position; independent variable for equations of motion
ω	angular frequency

Subscripts:

k	cavity number
mid	middle

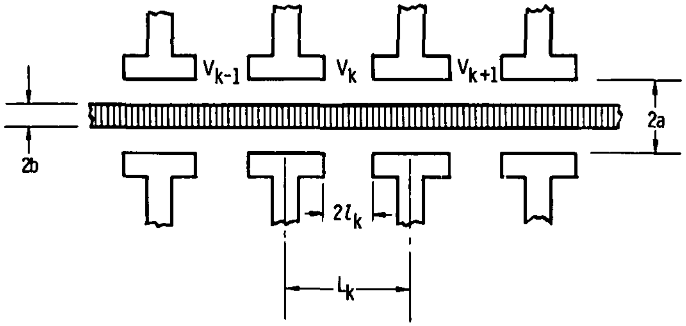

Figure 1. - Model of coupled-cavity traveling wave tube.

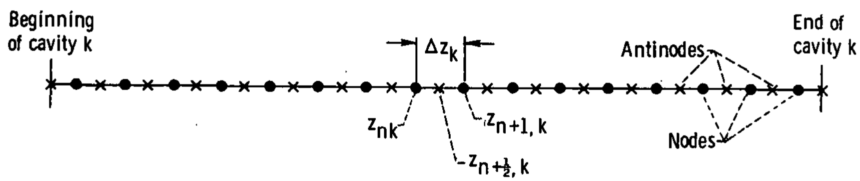

Figure 2. - Nodes and antinodes for cavity k.

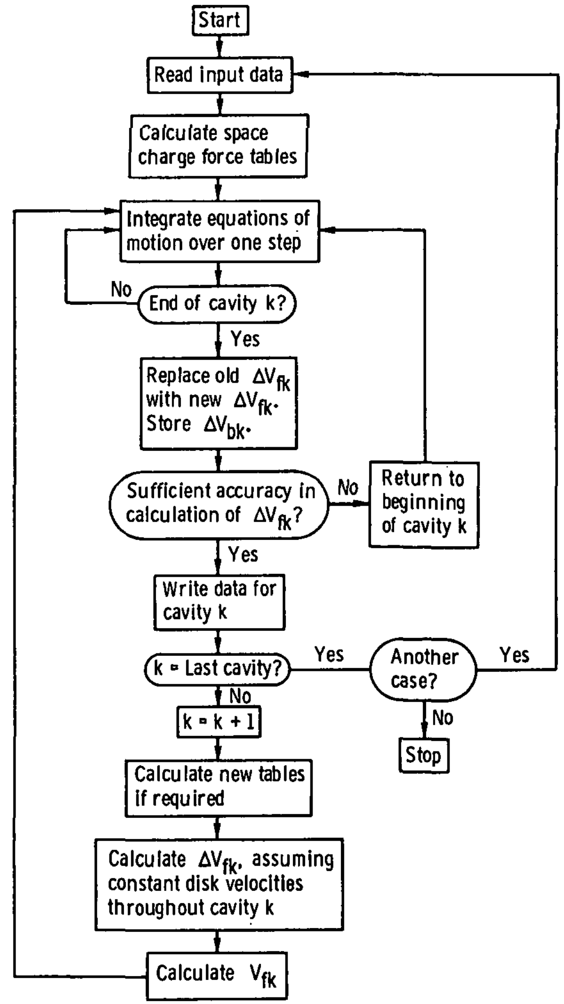

Figure 3. - Flow chart for computational procedure.

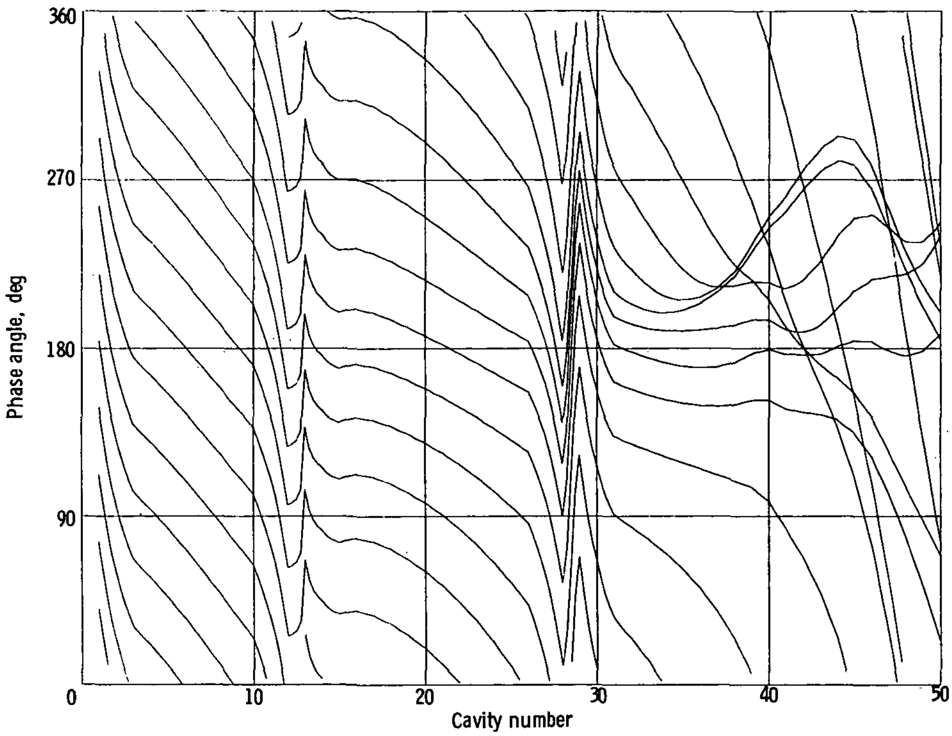

Figure 4. - Applegate diagram.

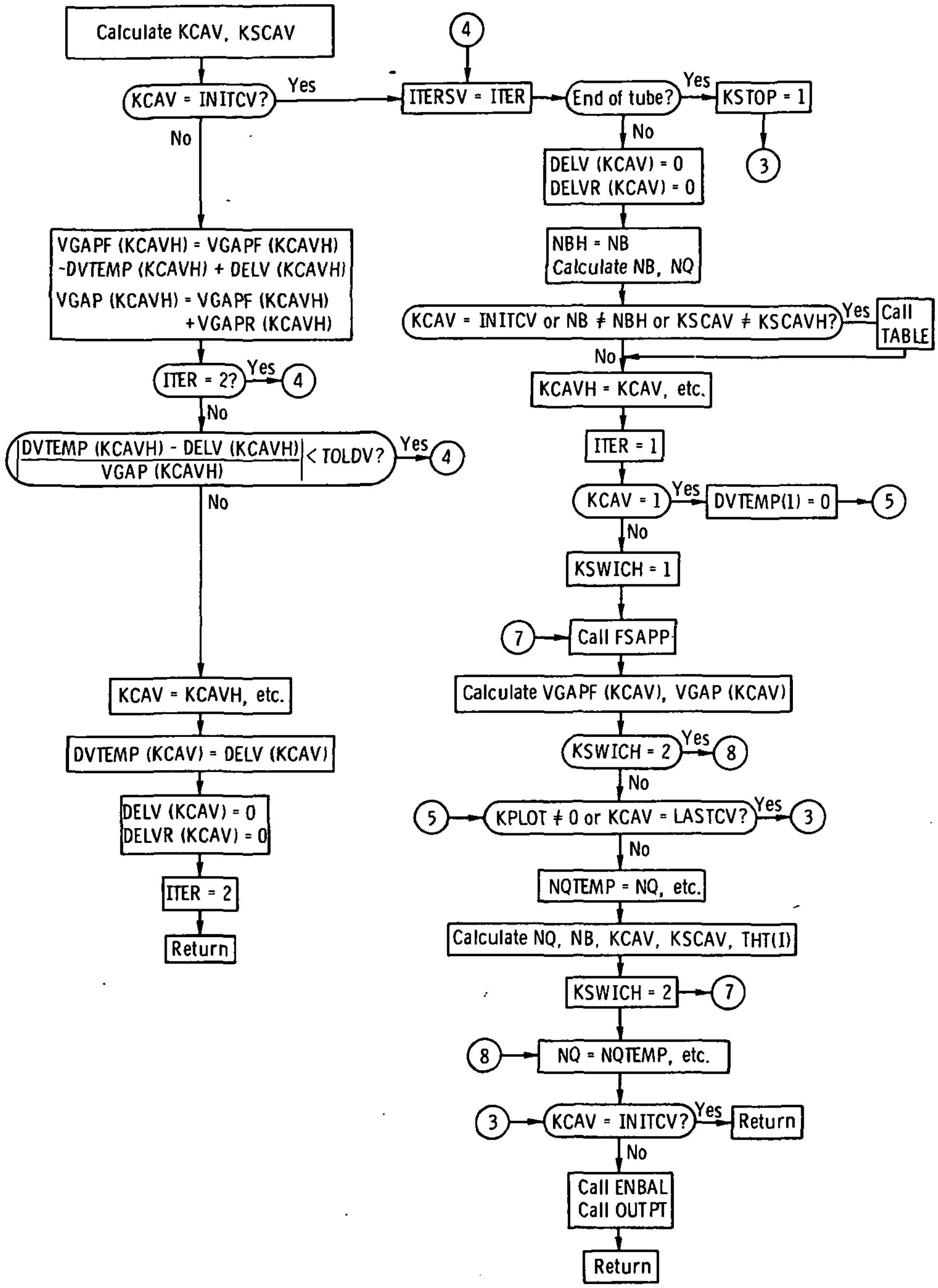

Figure 5. - Flow chart for subroutine BTWNC.

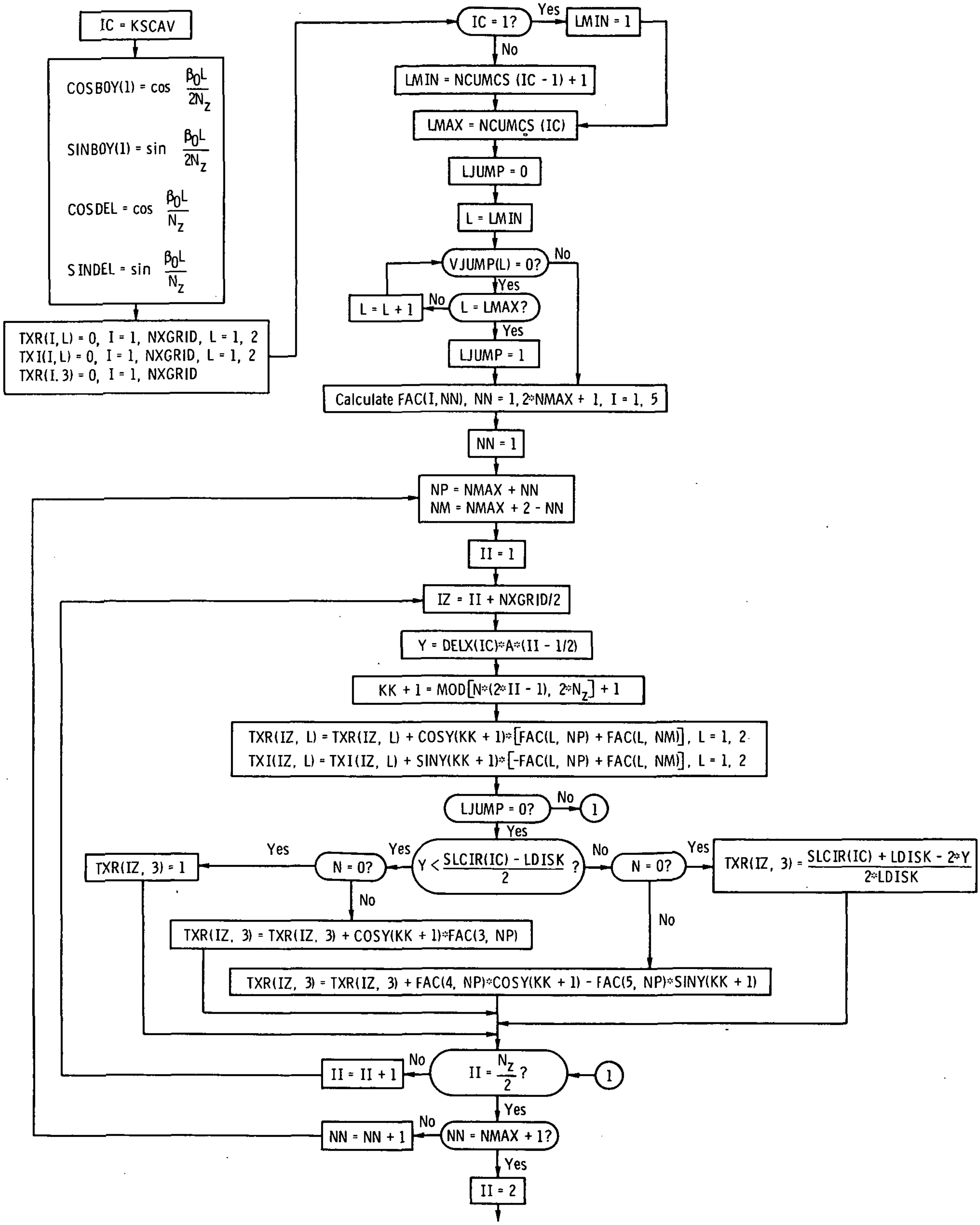

Figure 6. - Flow chart for subroutine TABLE.

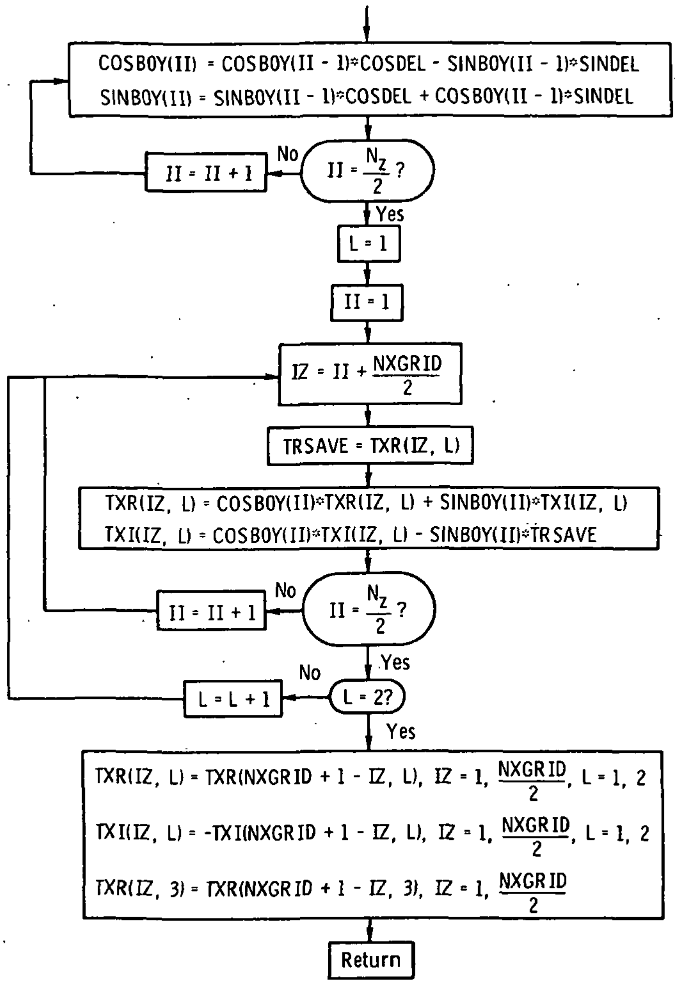

Figure 6. - Concluded.

APPENDIX B

SAMPLE PROGRAM RUN

A sample run, which illustrates the use of the program, is given in this appendix. The output of this run is given in figure 7. The input parameters are chosen to represent a tube with a lumped sever, a single-step circuit velocity reduction, and an accelerating voltage jump. This run also illustrates the use of the iterative procedure to calculate the effect of the backward wave on tube performance. This run is not intended to represent a finished tube design but to illustrate use of the various program capabilities.

A list of input parameters for the first case is followed by the output for the first case - a first iteration through the entire 37-cavity tube, ignoring the backward wave. Note that the tube is severed at cavities 13 and 14. Going from cavity 25 to cavity 26, we encounter a step reduction in circuit velocity. A voltage jump occurs at cavity 32. Figure 8 shows the Applegate diagram for this case.

The remaining nine cases illustrate the iterative procedure used to evaluate the effect of the backward wave. The output of each case is preceded by a list of those input parameters that are changed from the previous case.

Effectively, there are five iterations through the input section and five through the output section. Note that satisfactory convergence is achieved with three iterations in each section. Comparing the first case to the last shows the effect of the backward wave. A list of normalized final velocities of the disks in a beam wavelength is also included in the output for each case.

```
CASE NUMBER  1
ENTER ' &INPUT'
&INPUT
ACM= 0.6349999E-01
ALPHL= 12*0.50E-01, 0.350E03, 12*0.50E-01, 12*0.6999993E-01, 615*0.0
ALPHLR= 12*0.50E-01, 0.350E03, 12*0.50E-01, 12*0.6999993E-01, 615*0.0
B1LDP= 37*1.230, 615*0.0
BCM= 0.2860E-01, 2*0.0
COSHML= 1.0
DATTEN= 1.0, 2*0.0
FREQGH= 12.10
INITCV= 1
IOBMA= 75.0
ISAVE= 0
ISTATE= 1
JSCP= 16
KCYCLE= 0
KIMP= 1
KLOSS= 0
KPLOT= 0
KPRINT= 0
KREL= 0
KSMSIG= 0
KSPACE= 0
KVEL= 37, 651*0
LASTCV= 37
LCIRCM= 25*0.31750, 12*0.2539999, 615*0.0
LGAPCM= 25*0.9649998E-01, 12*0.7720E-01, 615*0.0
NA1= 0
NA2= 0
NB1= 0
NB2= 0
NBWM= 0
NCAVSS= 1
NDISKS= 24
NMAX= 5
NUMA= 1
NUMB= 1
NVEL= 1
NXGRID= 16
NXISC= 100
PINDBM= 30.0
SCMAX= 6.50
TOLDV= 0.250E-01
TOLSC= 0.250E-01
VOB= 11300.0
VJUMP= 31*0.0, 1000.0, 620*0.0
ZIMP= 25*2000.0, 12*1500.0, 615*0.0
IDEBUG= 500*0
&END

RATIO OF LARGEST SPACE CHARGE FORCE TO SMALLEST =  0.118E 03
```

Figure 7. - Output of sample program run.

UO	BEB	B1B	KP	ZC	C	B	D	DGAIN	QQ	A1+A2
0.6203E 08	0.3505E 00	0.3481E 00	0.9313E 02	0.2000E 04	0.5366E-01	-0.1312E 00	0.2756E-01	0.1362E 01	0.1338E 01	-0.9108E 01

CAV	VMAG	VPHA	ISMAG	ISPHA	VPHA-ISPHA	LS GAIN	POUT	EFF	PKE	PFW	PBW	PLC	PBAL	ITER	SC
1	0.63195E 02	-0.0001	0.0008	-0.8362	-0.8361	-0.0069	0.998	0.0012	0.00	0.00	0.00	0.00	1.000	1	16
2	0.62671E 02	0.7670	0.0079	0.1801	-0.5869	-0.0793	0.982	0.0012	0.01	-0.02	0.00	0.01	1.000	1	16
3	0.62019E 02	-0.4714	0.0222	0.9767	1.4481	-0.1702	0.962	0.0011	0.02	-0.04	0.00	0.02	1.000	1	16
4	0.61279E 02	0.2818	0.0434	-0.2474	-0.5293	-0.2744	0.939	0.0011	0.03	-0.06	0.00	0.03	1.000	1	16
5	0.60653E 02	-0.9760	0.0710	0.5216	1.4976	-0.3635	0.920	0.0011	0.05	-0.08	0.00	0.04	1.000	1	16
6	0.60626E 02	-0.2472	0.1044	-0.7136	-0.4664	-0.3674	0.919	0.0011	0.02	-0.08	0.00	0.05	1.000	1	16
7	0.62061E 02	0.4676	0.1430	0.0482	-0.4195	-0.1642	0.963	0.0011	-0.04	-0.04	0.00	0.07	1.000	1	16
8	0.66146E 02	-0.8284	0.1861	0.8071	1.6355	0.3894	1.094	0.0013	-0.20	0.10	0.00	0.08	1.000	1	16
9	0.74073E 02	-0.1287	0.2330	-0.4369	-0.3082	1.3726	1.372	0.0016	-0.51	0.37	0.00	0.09	1.000	1	16
10	0.86624E 02	0.5743	0.2829	0.3160	-0.2584	2.7322	1.876	0.0022	-1.06	0.88	0.00	0.10	1.000	1	16
11	0.10401E 03	-0.7151	0.3351	-0.9348	-0.2196	4.3212	2.705	0.0032	-1.95	1.71	0.00	0.13	1.000	1	16
12	0.12607E 03	0.0034	0.3894	-0.1895	-0.1930	5.9917	3.973	0.0047	-3.30	2.98	0.00	0.16	1.000	1	16
13	0.15247E 03	0.7284	0.4457	0.5512	-0.1772	7.6432	5.812	0.0069	-5.24	4.81	0.00	0.20	1.000	1	16
14	0.37884E 02	-0.7120	0.5051	-0.7120	0.0000	-4.4515	0.359	0.0004	-5.66	-0.64	0.00	6.01	1.000	1	8
15	0.79502E 02	0.0423	0.5590	0.0281	-0.0142	1.9869	1.580	0.0019	-6.96	0.58	0.00	6.02	1.000	1	8
16	0.12412E 03	0.7958	0.6049	0.7672	-0.0286	5.8565	3.852	0.0045	-9.31	2.85	0.00	6.04	1.000	1	8
17	0.17097E 03	-0.4519	0.6433	-0.4975	-0.0456	8.6378	7.308	0.0086	-12.85	6.31	0.00	6.08	0.999	1	8
18	0.21919E 03	0.2982	0.6754	0.2311	-0.0671	10.7958	12.011	0.0142	-17.69	11.01	0.00	6.16	0.999	1	8
19	0.26786E 03	-0.9544	0.7039	0.9509	1.9053	12.5374	17.937	0.0212	-23.80	16.94	0.00	6.30	0.999	1	8
20	0.31595E 03	-0.2103	0.7329	-0.3392	-0.1289	13.9719	24.957	0.0294	-31.10	23.96	0.00	6.51	0.999	1	8
21	0.36238E 03	0.5300	0.7675	0.3606	-0.1695	15.1626	32.829	0.0387	-39.35	31.83	0.00	6.79	0.999	1	8
22	0.40596E 03	-0.7336	0.8131	-0.9479	-0.2143	16.1491	41.201	0.0486	-48.25	40.20	0.00	7.17	0.999	1	2
23	0.44553E 03	-0.0014	0.8725	-0.2618	-0.2604	16.9569	49.624	0.0586	-57.35	48.63	0.00	7.64	0.999	1	2
24	0.47989E 03	0.7269	0.9438	0.4220	-0.3049	17.6023	57.574	0.0679	-66.14	56.58	0.00	8.21	0.998	1	1
25	0.50784E 03	-0.5483	1.0173	-0.8942	-0.3459	18.0939	64.475	0.0761	-73.87	63.48	0.00	8.87	0.998	1	1
26	0.47598E 03	0.1885	1.0906	-0.0780	-0.2665	18.7805	75.518	0.0891	-85.79	74.52	0.00	9.61	0.998	1	1
27	0.53270E 03	0.9474	1.1197	0.8639	-0.0836	19.7584	94.588	0.1116	-106.05	93.59	0.00	10.81	0.998	1	1
28	0.58949E 03	-0.2749	1.1118	-0.2094	0.0655	20.6383	115.832	0.1367	-128.58	114.83	0.00	12.33	0.998	1	1
29	0.63313E 03	0.5127	1.0469	0.6972	0.1845	21.2587	133.620	0.1577	-147.82	132.62	0.00	14.18	0.999	1	1
30	0.65929E 03	-0.6976	0.8997	-0.4191	0.2785	21.6104	144.889	0.1710	-160.80	143.89	0.00	16.31	0.999	1	1
31	0.67044E 03	0.0881	0.6504	0.4319	0.3438	21.7560	149.830	0.1768	-167.68	148.83	0.00	18.63	1.000	1	1
32	0.67460E 03	0.8660	0.3393	-0.8047	-1.6707	21.8098	151.697	0.1644	-96.90	150.70	0.00	21.03	1.000	1	1
33	0.68038E 03	-0.3627	0.2053	-0.2837	0.0789	21.8838	154.305	0.1673	-102.04	153.31	0.00	23.45	1.000	1	1
34	0.69294E 03	0.4053	0.3299	0.3297	-0.0755	22.0427	160.055	0.1735	-110.33	159.06	0.00	25.92	1.000	1	1
35	0.70800E 03	-0.8281	0.3897	-0.9365	-0.1084	22.2294	167.087	0.1811	-119.81	166.09	0.00	28.48	1.000	1	1
36	0.71802E 03	-0.0631	0.3408	-0.2550	-0.1920	22.3515	171.851	0.1863	-127.33	170.85	0.00	31.15	1.000	1	1
37	0.71746E 03	0.6995	0.3108	0.2994	-0.4001	22.3447	171.582	0.1860	-129.65	170.58	0.00	33.90	1.000	1	1

NORMALIZED VELOCITIES

1.11988	1.09214	1.07454	1.04653	1.05086	1.00619	0.97224	0.99819	0.98893	0.99158	0.99027	0.98127
0.93284	0.82011	0.72483	0.69099	0.70851	0.71631	0.72578	0.72045	0.71740	0.70768	1.00748	1.03800

CASE NUMBER 2
ENTER ' &INPUT'

&INPUT LASTCV=13, NBWM=13,KSMSIG=1,KPRINT=1, KPLOT=1 &END

RATIO OF LARGEST SPACE CHARGE FORCE TO SMALLEST = 0.118E 03

Figure 7. - Continued.

CAV	VMAG	VPHA	ISMAG	ISPHA	VPHA-ISPHA	LS GAIN	POUT	EFF	PKE	PFW	PBW	PLC	PBAL	ITER	SC
1	0.87180E 02	0.0080	0.0011	-0.8269	-0.8350	-0.0094	0.998	0.0012	0.00	0.00	-0.15	0.00	1.000	1	16
2	0.67586E 02	0.8826	0.0109	0.1999	-0.6827	-0.0833	0.981	0.0012	0.02	-0.02	-0.16	0.01	1.000	1	16
3	0.37508E 02	-0.4504	0.0280	-0.9786	-0.5282	-0.1416	0.968	0.0011	0.03	-0.03	-0.16	0.03	1.000	1	16
4	0.60895E 02	0.1452	0.0490	-0.2008	-0.3460	-0.1696	0.962	0.0011	-0.02	-0.04	-0.12	0.04	1.000	1	16
5	0.83303E 02	0.9914	0.0755	0.5530	-0.4383	-0.1661	0.962	0.0011	-0.04	-0.04	-0.11	0.05	1.000	1	16
6	0.67344E 02	-0.1538	0.1104	-0.6934	-0.5396	-0.0691	0.984	0.0012	0.00	-0.01	-0.21	0.07	1.000	1	16
7	0.36231E 02	0.4500	0.1513	0.0679	-0.3821	0.2680	1.064	0.0013	-0.01	0.07	-0.28	0.08	1.000	1	16
8	0.71553E 02	-0.9838	0.1934	0.8285	1.8123	0.9590	1.247	0.0015	-0.35	0.25	-0.14	0.09	1.000	1	16
9	0.10129E 03	-0.1630	0.2367	-0.4185	-0.2555	1.9982	1.584	0.0019	-0.85	0.59	-0.03	0.11	1.000	1	16
10	0.89489E 02	0.6207	0.2849	0.3295	-0.2912	3.3189	2.147	0.0025	-1.22	1.15	-0.27	0.13	1.000	1	16
11	0.86473E 02	-0.7769	0.3366	-0.9227	-0.1458	4.8278	3.039	0.0036	-1.92	2.04	-0.51	0.16	1.000	1	16
12	0.14350E 03	-0.0845	0.3873	-0.1769	-0.0924	6.4009	4.366	0.0052	-3.53	3.37	-0.28	0.20	1.000	1	16
13	0.18641E 03	0.7114	0.4368	0.5620	-0.1494	7.9372	6.219	0.0073	-5.77	5.22	0.00	0.25	1.000	1	16

CASE NUMBER 3
ENTER ' &INPUT'
&INPUT &END

RATIO OF LARGEST SPACE CHARGE FORCE TO SMALLEST = 0.118E 03

CAV	VMAG	VPHA	ISMAG	ISPHA	VPHA-ISPHA	LS GAIN	POUT	EFF	PKE	PFW	PBW	PLC	PBAL	ITER	SC
1	0.86320E 02	0.0167	0.0011	-0.8182	-0.8349	-0.0091	0.998	0.0012	0.00	0.00	-0.14	0.00	1.000	1	16
2	0.65086E 02	0.8839	0.0108	0.2085	-0.6753	-0.0798	0.982	0.0012	0.02	-0.02	-0.15	0.01	1.000	1	16
3	0.37677E 02	-0.4712	0.0275	-0.9726	-0.5014	-0.1326	0.970	0.0011	0.02	-0.03	-0.15	0.03	1.000	1	16
4	0.62868E 02	0.1493	0.0482	-0.1976	-0.3468	-0.1564	0.965	0.0011	-0.02	-0.03	-0.11	0.04	1.000	1	16
5	0.83069E 02	0.9979	0.0745	0.5548	-0.4431	-0.1513	0.966	0.0011	-0.04	-0.03	-0.10	0.05	1.000	1	16
6	0.65527E 02	-0.1535	0.1093	-0.6918	-0.5383	-0.0547	0.987	0.0012	-0.00	-0.01	-0.21	0.07	1.000	1	16
7	0.36966E 02	0.4330	0.1498	0.0694	-0.3636	0.2770	1.066	0.0013	-0.02	0.07	-0.28	0.08	1.000	1	16
8	0.73162E 02	-0.9781	0.1915	0.8296	1.8077	0.9538	1.246	0.0015	-0.36	0.25	-0.14	0.09	1.000	1	16
9	0.10092E 03	-0.1578	0.2347	-0.4178	-0.2600	1.9738	1.575	0.0019	-0.84	0.58	-0.03	0.11	1.000	1	16
10	0.88494E 02	0.6203	0.2827	0.3300	-0.2903	3.2773	2.127	0.0025	-1.21	1.13	-0.26	0.13	1.000	1	16
11	0.87455E 02	-0.7775	0.3342	-0.9222	-0.1447	4.7736	3.002	0.0035	-1.92	2.00	-0.50	0.16	1.000	1	16
12	0.14383E 03	-0.0801	0.3846	-0.1766	-0.0966	6.3383	4.304	0.0051	-3.52	3.31	-0.27	0.19	1.000	1	16
13	0.18507E 03	0.7149	0.4341	0.5621	-0.1528	7.8702	6.124	0.0072	-5.71	5.13	0.00	0.24	1.000	1	16

CASE NUMBER 4
ENTER ' &INPUT'
&INPUT &END

RATIO OF LARGEST SPACE CHARGE FORCE TO SMALLEST = 0.118E 03

CAV	VMAG	VPHA	ISMAG	ISPHA	VPHA-ISPHA	LS GAIN	POUT	EFF	PKE	PFW	PBW	PLC	PBAL	ITER	SC
1	0.86078E 02	0.0165	0.0010	-0.8185	-0.8350	-0.0091	0.998	0.0012	0.00	0.00	-0.14	0.00	1.000	1	16
2	0.65039E 02	0.8827	0.0107	0.2082	-0.6744	-0.0799	0.982	0.0012	0.02	-0.02	-0.15	0.01	1.000	1	16
3	0.37930E 02	-0.4712	0.0274	-0.9731	-0.5019	-0.1331	0.970	0.0011	0.02	-0.03	-0.15	0.03	1.000	1	16
4	0.62820E 02	0.1504	0.0481	-0.1981	-0.3485	-0.1578	0.964	0.0011	-0.02	-0.03	-0.11	0.04	1.000	1	16
5	0.82899E 02	0.9980	0.0744	0.5544	-0.4437	-0.1539	0.965	0.0011	-0.04	-0.03	-0.10	0.05	1.000	1	16
6	0.65499E 02	-0.1543	0.1092	-0.6921	-0.5378	-0.0586	0.987	0.0012	-0.00	-0.01	-0.20	0.07	1.000	1	16
7	0.37183E 02	0.4336	0.1498	0.0691	-0.3645	0.2713	1.064	0.0013	-0.02	0.07	-0.27	0.08	1.000	1	16
8	0.73061E 02	-0.9771	0.1915	0.8293	1.8064	0.9469	1.244	0.0015	-0.36	0.25	-0.14	0.09	1.000	1	16
9	0.10074E 03	-0.1577	0.2347	-0.4181	-0.2604	1.9665	1.573	0.0019	-0.84	0.57	-0.03	0.11	1.000	1	16
10	0.88477E 02	0.6200	0.2827	0.3298	-0.2902	3.2706	2.124	0.0025	-1.21	1.13	-0.25	0.13	1.000	1	16
11	0.87538E 02	-0.7771	0.3342	-0.9225	-0.1453	4.7680	2.998	0.0035	-1.92	2.00	-0.49	0.16	1.000	1	16

Figure 7. - Continued.

12	0.14368E 03	-0.0797	0.3847	-0.1769	-0.0971	6.3339	4.299	0.0051	-3.52	3.30	-0.27	0.19	1.000	1	16
13	0.18486E 03	0.7148	0.4342	0.5619	-0.1529	7.8671	6.119	0.0072	-5.71	5.12	0.00	0.24	1.000	1	16

CASE NUMBER 5
ENTER ' &INPUT'

&INPUT INITCV=14, LASTCV=37, ISTATE=2 &END

CAV	VMAG	VPHA	ISMAG	ISPHA	VPHA-ISPHA	LS GAIN	POUT	EFF	PKE	PFW	PBW	PLC	PBAL	ITER	SC
14	0.36625E 02	-0.7049	0.4883	-0.7049	0.0000	-4.7452	0.335	0.0004	-6.10	-0.66	0.00	6.36	1.000	1	16
15	0.76665E 02	0.0477	0.5381	0.0320	-0.0157	1.6713	1.469	0.0017	-7.30	0.47	0.00	6.37	0.999	1	16
16	0.11946E 03	0.7998	0.5808	0.7684	-0.0314	5.5235	3.567	0.0042	-9.47	2.57	0.00	6.38	0.999	1	8
17	0.16427E 03	-0.4494	0.6170	-0.4988	-0.0494	8.2908	6.746	0.0080	-12.74	5.75	0.00	6.42	0.999	1	8
18	0.21035E 03	0.2995	0.6480	0.2279	-0.0716	10.4381	11.061	0.0131	-17.18	10.06	0.00	6.50	0.999	1	8
19	0.25683E 03	-0.9543	0.6764	0.9463	1.9006	12.1723	16.491	0.0195	-22.79	15.49	0.00	6.63	0.999	1	8
20	0.30283E 03	-0.2112	0.7063	-0.3447	-0.1335	13.6032	22.926	0.0271	-29.48	21.93	0.00	6.82	0.999	1	8
21	0.34736E 03	0.5283	0.7427	0.3551	-0.1732	14.7951	30.165	0.0356	-37.08	29.17	0.00	7.08	0.999	1	8
22	0.38945E 03	-0.7361	0.7903	-0.9525	-0.2164	15.7884	37.918	0.0447	-45.32	36.92	0.00	7.42	0.999	1	4
23	0.42809E 03	-0.0045	0.8518	-0.2648	-0.2603	16.6100	45.815	0.0541	-53.85	44.82	0.00	7.86	0.999	1	2
24	0.46228E 03	0.7231	0.9253	0.4210	-0.3022	17.2776	53.427	0.0630	-62.27	52.43	0.00	8.38	0.998	1	1
25	0.49098E 03	-0.5527	1.0019	-0.8932	-0.3405	17.8006	60.265	0.0711	-69.91	59.27	0.00	8.99	0.998	1	1
26	0.46210E 03	0.1841	1.0785	-0.0751	-0.2592	18.5234	71.178	0.0840	-81.65	70.18	0.00	9.68	0.998	1	1
27	0.51894E 03	0.9439	1.1116	0.8687	-0.0752	19.5311	89.766	0.1059	-101.39	88.77	0.00	10.82	0.998	1	1
28	0.57522E 03	-0.2771	1.1092	-0.2018	0.0753	20.4255	110.294	0.1301	-123.16	109.30	0.00	12.26	0.998	1	1
29	0.61775E 03	0.5121	1.0523	0.7094	0.1973	21.0450	127.206	0.1501	-141.45	126.21	0.00	14.02	0.999	1	1
30	0.64198E 03	-0.6963	0.9164	-0.3986	0.2977	21.3793	137.381	0.1621	-153.19	136.38	0.00	16.05	0.999	1	1
31	0.64993E 03	0.0914	0.6781	0.4710	0.3796	21.4861	140.803	0.1661	-158.43	139.80	0.00	18.25	1.000	1	1
32	0.64926E 03	0.8710	0.3562	-0.7067	-1.5778	21.4772	140.515	0.1523	-85.29	139.52	0.00	20.50	1.000	1	1
33	0.64926E 03	-0.3571	0.1140	-0.1596	0.1975	21.4771	140.512	0.1523	-87.61	139.51	0.00	22.75	1.000	1	1
34	0.65779E 03	0.4102	0.2625	0.2921	-0.1181	21.5905	144.227	0.1563	-93.68	143.23	0.00	25.00	1.000	1	1
35	0.67259E 03	-0.8235	0.3834	-0.9402	-0.1166	21.7838	150.794	0.1635	-102.48	149.80	0.00	27.30	1.000	1	1
36	0.68603E 03	-0.0577	0.3699	-0.1951	-0.1374	21.9557	156.881	0.1701	-111.05	155.88	0.00	29.71	1.000	1	1
37	0.69084E 03	0.7067	0.2830	0.4339	-0.2728	22.0164	159.088	0.1725	-115.62	158.09	0.00	32.22	1.000	1	1

NORMALIZED VELOCITIES

1.11726	1.08947	1.07372	1.04696	1.05774	1.01728	0.96879	0.99360	1.00228	0.99244	0.99023	0.98204
0.97339	0.90965	0.79293	0.72563	0.69675	0.71311	0.72617	0.72703	0.71229	0.70759	0.99442	1.04434

CASE NUMBER 6
ENTER ' &INPUT'

&INPUT NBWM=37, ISTATE=1 &END

CAV	VMAG	VPHA	ISMAG	ISPHA	VPHA-ISPHA	LS GAIN	POUT	EFF	PKE	PFW	PBW	PLC	PBAL	ITER	SC
14	0.69402E 02	-0.9205	0.4881	-0.7046	0.2159	-4.7487	0.335	0.0004	-6.08	-0.66	-0.58	6.36	0.999	1	8
15	0.12069E 03	-0.0121	0.5333	0.0325	0.0445	1.6290	1.455	0.0017	-7.71	0.46	-0.11	6.37	0.999	1	8
16	0.13903E 03	0.8001	0.5698	0.7668	-0.0333	5.4340	3.495	0.0041	-9.79	2.50	-0.14	6.39	0.999	1	8
17	0.15746E 03	-0.4964	0.6010	-0.5024	-0.0061	8.1584	6.544	0.0077	-12.34	5.55	-0.75	6.44	0.999	1	8
18	0.22518E 03	0.2222	0.6255	0.2237	0.0015	10.2620	10.622	0.0125	-16.52	9.62	-0.77	6.52	0.999	1	8
19	0.29339E 03	-0.9965	0.6433	0.9407	1.9372	11.9408	15.634	0.0184	-22.30	14.64	-0.14	6.64	0.999	1	8
20	0.31446E 03	-0.2220	0.6622	-0.3545	-0.1325	13.3039	21.399	0.0252	-28.21	20.40	-0.23	6.83	0.999	1	8
21	0.32049E 03	0.4989	0.6918	0.3409	-0.1580	14.4250	27.701	0.0327	-34.20	26.70	-0.97	7.09	0.998	1	8
22	0.37278E 03	-0.7927	0.7338	-0.9691	-0.1764	15.3499	34.276	0.0404	-41.48	33.28	-0.78	7.41	0.998	1	4

Figure 7. - Continued.

23	0.43173E 03	-0.0453	0.7888	-0.2833	-0.2380	16.1031	40.768	0.0481	-49.18	39.77	-0.10	7.81	0.998	1	2
24	0.43695E 03	0.7042	0.8599	0.4012	-0.3030	16.7058	46.836	0.0553	-55.44	45.84	-0.70	8.29	0.998	1	2
25	0.42300E 03	-0.5875	0.9401	-0.9107	-0.3231	17.1821	52.265	0.0617	-60.93	51.27	-1.55	8.85	0.997	1	1
26	0.41038E 03	0.1278	1.0198	-0.0876	-0.2154	17.8985	61.638	0.0727	-71.00	60.64	-1.70	9.48	0.997	1	1
27	0.50219E 03	0.8924	1.0566	0.8620	-0.0303	18.9280	78.128	0.0922	-88.39	77.13	-1.91	10.50	0.997	1	1
28	0.58899E 03	-0.3143	1.0588	-0.2006	0.1138	19.8376	96.331	0.1137	-107.73	95.33	-1.92	11.77	0.997	1	1
29	0.64807E 03	0.4948	1.0100	0.7215	0.2268	20.4466	110.832	0.1308	-123.74	109.83	-1.52	13.33	0.998	1	1
30	0.66302E 03	-0.6936	0.8888	-0.3702	0.3234	20.7359	118.464	0.1398	-133.27	117.47	-0.81	15.10	0.998	1	1
31	0.63831E 03	0.1065	0.6735	0.5291	0.4225	20.7576	119.059	0.1405	-135.81	118.06	-0.24	17.00	0.999	1	1
32	0.60043E 03	0.8860	0.3728	-0.5677	-1.4537	20.6254	115.489	0.1252	-59.23	114.49	-0.02	18.90	0.999	1	1
33	0.57677E 03	-0.3521	0.0735	0.4936	0.8457	20.5004	112.212	0.1216	-57.78	111.21	-0.03	20.75	0.999	1	1
34	0.58009E 03	0.4050	0.2091	0.1651	-0.2399	20.5562	113.664	0.1232	-61.13	112.67	-0.11	22.54	0.999	1	1
35	0.59965E 03	-0.8338	0.3593	-0.9305	-0.0967	20.7673	119.325	0.1293	-68.56	118.33	-0.17	24.36	0.999	1	1
36	0.62170E 03	-0.0657	0.3524	-0.0873	-0.0215	20.9811	125.347	0.1359	-76.44	124.35	-0.09	26.27	0.999	1	1
37	0.63058E 03	0.7072	0.2141	0.6416	-0.0656	21.0771	128.147	0.1389	-81.23	127.15	0.00	28.28	0.999	1	1

NORMALIZED VELOCITIES

```
1.11557  1.08623  1.06070  1.03640  1.05463  1.05747  1.03402  0.98458  0.99179  0.99932  0.98624  0.98032
0.98485  0.99400  0.94959  0.87648  0.76971  0.71319  0.72962  0.74467  0.71393  0.72695  0.97694  1.05212
```

CASE NUMBER 7
ENTER ' &INPUT'
&INPUT &END

CAV	VMAG	VPHA	ISMAG	ISPHA	VPHA-ISPHA	LS GAIN	POUT	EFF	PKE	PPW	PBW	PLC	PBAL	ITER	SC
14	0.83930E 02	-0.8912	0.4879	-0.7046	0.1866	-4.7521	0.335	0.0004	-6.38	-0.66	-0.55	6.36	0.999	1	8
15	0.12277E 03	0.0297	0.5328	0.0311	0.0015	1.6224	1.453	0.0017	-8.08	0.45	-0.02	6.37	0.999	1	8
16	0.12374E 03	0.8130	0.5710	0.7642	-0.0488	5.4347	3.495	0.0041	-9.82	2.50	-0.38	6.40	0.998	1	8
17	0.15420E 03	-0.5293	0.6045	-0.5049	0.0244	8.1717	6.564	0.0077	-12.32	5.57	-1.06	6.45	0.998	1	8
18	0.24074E 03	0.2171	0.6295	0.2217	0.0045	10.2842	10.676	0.0126	-16.92	9.68	-0.69	6.52	0.998	1	8
19	0.29942E 03	-0.9812	0.6472	0.9381	1.9193	11.9675	15.731	0.0186	-22.81	14.73	-0.01	6.65	0.998	1	8
20	0.30043E 03	-0.2142	0.6682	-0.3578	-0.1436	13.3363	21.559	0.0254	-28.38	20.56	-0.51	6.84	0.998	1	8
21	0.31315E 03	0.4841	0.6999	0.3385	-0.1455	14.4667	27.968	0.0330	-34.47	26.97	-1.18	7.10	0.998	1	8
22	0.38738E 03	-0.7984	0.7418	-0.9706	-0.1722	15.4005	34.678	0.0409	-42.29	33.68	-0.53	7.42	0.998	1	4
23	0.43967E 03	-0.0353	0.7964	-0.2852	-0.2499	16.1593	41.298	0.0487	-49.96	40.30	-0.05	7.83	0.998	1	2
24	0.42431E 03	0.7102	0.8685	0.3992	-0.3110	16.7672	47.503	0.0561	-55.83	46.51	-1.13	8.32	0.997	1	2
25	0.41749E 03	-0.5983	0.9486	-0.9119	-0.3137	17.2506	53.096	0.0626	-61.70	52.10	-1.62	8.88	0.997	1	1
26	0.42508E 03	0.1235	1.0263	-0.0890	-0.2124	17.9696	62.656	0.0739	-72.42	61.66	-1.20	9.51	0.997	1	1
27	0.51117E 03	0.8993	1.0612	0.8598	-0.0395	18.9955	79.350	0.0936	-90.24	78.35	-1.14	10.53	0.997	1	1
28	0.57970E 03	-0.3107	1.0624	-0.2041	0.1066	19.9017	97.763	0.1154	-109.51	96.77	-1.46	11.83	0.997	1	1
29	0.63863E 03	0.4883	1.0134	0.7168	0.2285	20.5113	112.495	0.1327	-125.25	111.50	-1.73	13.42	0.998	1	1
30	0.67287E 03	-0.7024	0.8909	-0.3759	0.3265	20.8039	120.336	0.1420	-134.80	119.34	-1.46	15.23	0.998	1	1
31	0.65879E 03	0.1064	0.6707	0.5220	0.4155	20.8310	121.089	0.1429	-137.81	120.09	-0.77	17.16	0.998	1	1
32	0.60510E 03	0.8943	0.3615	-0.5803	-1.4746	20.7095	117.746	0.1276	-61.80	116.75	-0.29	19.09	0.999	1	1
33	0.56274E 03	-0.3505	0.0520	0.4576	0.8081	20.6031	114.898	0.1246	-60.86	113.90	-0.22	20.98	0.999	1	1
34	0.57542E 03	0.3953	0.2208	0.1910	-0.2043	20.6757	116.835	0.1267	-64.71	115.84	-0.26	22.82	0.999	1	1
35	0.61540E 03	-0.8413	0.3625	-0.9218	-0.0805	20.8890	122.716	0.1330	-72.52	121.72	-0.19	24.69	0.999	1	1
36	0.64016E 03	-0.0654	0.3417	-0.0928	-0.0274	21.0904	128.540	0.1393	-80.38	127.54	-0.05	26.65	0.999	1	1
37	0.63878E 03	0.7082	0.2040	0.5927	-0.1154	21.1699	130.916	0.1419	-84.80	129.92	0.00	28.71	0.999	1	1

NORMALIZED VELOCITIES

```
1.11805  1.08884  1.06199  1.03523  1.05514  1.05805  1.03391  0.98203  0.99133  0.99642  0.98320  0.97958
```

Figure 7. - Continued.

0.98537	0.99222	0.94115	0.85524	0.75481	0.71272	0.72861	0.74340	0.71358	0.71901	0.97658	1.05228

CASE NUMBER 8
ENTER ' &INPUT'
&INPUT &END

CAV	VMAG	VPHA	ISMAG	ISPHA	VPHA-ISPHA	LS GAIN	POUT	EFF	PKE	PFW	PBW	PLC	PBAL	ITER	SC
14	0.80007E 02	-0.8768	0.4880	-0.7046	0.1721	-4.7513	0.335	0.0004	-6.35	-0.66	-0.44	6.36	0.999	1	8
15	0.11752E 03	0.0263	0.5334	0.0312	0.0049	1.6279	1.455	0.0017	-7.95	0.46	-0.01	6.37	0.999	1	8
16	0.12418E 03	0.7994	0.5720	0.7648	-0.0345	5.4442	3.503	0.0041	-9.72	2.50	-0.36	6.40	0.999	1	8
17	0.15923E 03	-0.5262	0.6051	-0.5039	0.0223	8.1820	6.580	0.0078	-12.33	5.58	-0.91	6.44	0.999	1	8
18	0.23954E 03	0.2240	0.6298	0.2227	-0.0012	10.2942	10.701	0.0126	-16.90	9.70	-0.57	6.52	0.999	1	8
19	0.29440E 03	-0.9812	0.6478	0.9392	1.9204	11.9780	15.769	0.0186	-22.68	14.77	-0.01	6.65	0.998	1	8
20	0.30029E 03	-0.2192	0.6687	-0.3562	-0.1370	13.3479	21.617	0.0255	-28.32	20.62	-0.47	6.84	0.998	1	8
21	0.31837E 03	0.4849	0.6997	0.3403	-0.1446	14.4786	28.045	0.0331	-34.52	27.05	-1.03	7.09	0.998	1	8
22	0.38712E 03	-0.7935	0.7411	-0.9691	-0.1755	15.4115	34.765	0.0410	-42.26	33.77	-0.46	7.41	0.998	1	4
23	0.43486E 03	-0.0344	0.7958	-0.2837	-0.2493	16.1697	41.397	0.0488	-49.84	40.40	-0.08	7.82	0.998	1	2
24	0.42426E 03	0.7076	0.8678	0.4009	-0.3068	16.7775	47.615	0.0562	-55.84	46.62	-1.04	8.31	0.998	1	2
25	0.42235E 03	-0.5967	0.9475	-0.9104	-0.3138	17.2599	53.210	0.0628	-61.78	52.21	-1.44	8.88	0.997	1	1
26	0.42447E 03	0.1280	1.0255	-0.0876	-0.2156	17.9771	62.765	0.0741	-72.37	61.77	-1.13	9.51	0.997	1	1
27	0.50682E 03	0.9006	1.0610	0.8611	-0.0395	19.0017	79.465	0.0938	-90.01	78.47	-1.24	10.54	0.997	1	1
28	0.57873E 03	-0.3118	1.0628	-0.2026	0.1092	19.9077	97.897	0.1155	-109.18	96.90	-1.66	11.84	0.998	1	1
29	0.64242E 03	0.4885	1.0140	0.7187	0.2302	20.5166	112.633	0.1329	-124.96	111.63	-1.85	13.42	0.998	1	1
30	0.67570E 03	-0.6999	0.8915	-0.3736	0.3262	20.8079	120.445	0.1421	-134.57	119.45	-1.43	15.24	0.998	1	1
31	0.65692E 03	0.1090	0.6712	0.5244	0.4154	20.8335	121.158	0.1430	-137.58	120.16	-0.67	17.17	0.999	1	1
32	0.60216E 03	0.8945	0.3625	-0.5774	-1.4719	20.7106	117.777	0.1277	-61.50	116.78	-0.22	19.11	0.999	1	1
33	0.56438E 03	-0.3512	0.0544	0.4618	0.8130	20.6024	114.879	0.1245	-60.50	113.88	-0.18	20.99	0.999	1	1
34	0.57916E 03	0.3970	0.2183	0.1896	-0.2074	20.6723	116.744	0.1266	-64.31	115.75	-0.22	22.83	0.999	1	1
35	0.61543E 03	-0.8382	0.3606	-0.9224	-0.0842	20.8836	122.564	0.1329	-72.05	121.57	-0.15	24.70	0.999	1	1
36	0.63738E 03	-0.0637	0.3423	-0.0931	-0.0294	21.0855	128.395	0.1392	-79.90	127.40	-0.05	26.66	0.999	1	1
37	0.63753E 03	0.7089	0.2069	0.5976	-0.1113	21.1678	130.853	0.1418	-84.40	129.85	0.00	28.71	0.999	1	1

NORMALIZED VELOCITIES

1.11773	1.08879	1.06173	1.03503	1.05523	1.05807	1.03301	0.98211	0.99126	0.99724	0.98399	0.97970
0.98541	0.99317	0.94199	0.85791	0.75687	0.71269	0.72883	0.74379	0.71351	0.71965	0.97624	1.05183

CASE NUMBER 9
ENTER ' &INPUT'
&INPUT &END

CAV	VMAG	VPHA	ISMAG	ISPHA	VPHA-ISPHA	LS GAIN	POUT	EFF	PKE	PFW	PBW	PLC	PBAL	ITER	SC
14	0.79704E 02	-0.8803	0.4880	-0.7046	0.1756	-4.7513	0.335	0.0004	-6.34	-0.66	-0.45	6.36	0.999	1	8
15	0.11811E 03	0.0244	0.5333	0.0313	0.0069	1.6275	1.455	0.0017	-7.95	0.46	-0.01	6.37	0.999	1	8
16	0.12497E 03	0.8005	0.5718	0.7649	-0.0356	5.4428	3.502	0.0041	-9.73	2.50	-0.34	6.40	0.999	1	8
17	0.15870E 03	-0.5249	0.6048	-0.5039	0.0210	8.1798	6.576	0.0078	-12.33	5.58	-0.91	6.44	0.999	1	8
18	0.23894E 03	0.2233	0.6295	0.2227	-0.0006	10.2914	10.694	0.0126	-16.89	9.70	-0.59	6.52	0.999	1	8
19	0.29483E 03	-0.9819	0.6474	0.9392	1.9211	11.9748	15.757	0.0186	-22.68	14.76	-0.02	6.65	0.998	1	8
20	0.30106E 03	-0.2188	0.6683	-0.3563	-0.1375	13.3442	21.599	0.0255	-28.32	20.60	-0.46	6.84	0.998	1	8
21	0.31800E 03	0.4856	0.6993	0.3401	-0.1455	14.4742	28.017	0.0331	-34.50	27.02	-1.04	7.09	0.998	1	8
22	0.38646E 03	-0.7939	0.7408	-0.9692	-0.1754	15.4067	34.727	0.0410	-42.23	33.73	-0.48	7.41	0.998	1	4

Figure 7. - Continued.

```
23 0.43517E 03  -0.0349 0.7955  -0.2839  -0.2490   16.1646   41.349  0.0488  -49.82  40.35   -0.07   7.82 0.998    1   2
24 0.42486E 03   0.7078 0.8675   0.4007  -0.3071   16.7721   47.556  0.0561  -55.81  46.56   -1.03   8.31 0.998    1   2
25 0.42190E 03  -0.5963 0.9473  -0.9106  -0.3143   17.2543   53.142  0.0627  -61.73  52.14   -1.46   8.88 0.997    1   1
26 0.42392E 03   0.1276 1.0254  -0.0878  -0.2154   17.9717   62.686  0.0740  -72.31  61.69   -1.16   9.50 0.997    1   1
27 0.50709E 03   0.9002 1.0608   0.8610  -0.0392   18.9968   79.375  0.0937  -89.96  78.38   -1.25  10.53 0.997    1   1
28 0.57929E 03  -0.3117 1.0626  -0.2027   0.1090   19.9031   97.794  0.1154 -109.16  96.80   -1.64  11.83 0.997    1   1
29 0.64227E 03   0.4889 1.0138   0.7186   0.2297   20.5123  112.520  0.1328 -124.95 111.52   -1.83  13.42 0.998    1   1
30 0.67489E 03  -0.6997 0.8913  -0.3738   0.3260   20.8038  120.331  0.1420 -134.56 119.33   -1.42  15.23 0.998    1   1
31 0.65633E 03   0.1089 0.6713   0.5242   0.4154   20.8296  121.048  0.1428 -137.57 120.05   -0.67  17.15 0.999    1   1
32 0.60215E 03   0.8944 0.3628  -0.5776  -1.4720   20.7067  117.671  0.1276  -61.49 116.67   -0.23  19.09 0.999    1   1
33 0.56426E 03  -0.3511 0.0548   0.4606   0.8117   20.5983  114.770  0.1244  -60.48 113.77   -0.18  20.98 0.999    1   1
34 0.57848E 03   0.3971 0.2179   0.1894  -0.2077   20.6680  116.627  0.1264  -64.28 115.63   -0.22  22.82 0.999    1   1
35 0.61482E 03  -0.8384 0.3604  -0.9225  -0.0841   20.8792  122.440  0.1327  -72.01 121.44   -0.16  24.68 0.999    1   1
36 0.63724E 03  -0.0638 0.3421  -0.0929  -0.0291   21.0811  128.267  0.1390  -79.85 127.27   -0.05  26.64 0.999    1   1
37 0.63744E 03   0.7089 0.2068   0.5979  -0.1110   21.1635  130.723  0.1417  -84.35 129.73    0.00  28.69 0.999    1   1

NORMALIZED VELOCITIES
   1.11768    1.08869    1.06167    1.03505    1.05527    1.05813    1.03323    0.98214    0.99125    0.99720    0.98396    0.97964
   0.98541    0.99306    0.94215    0.85819    0.75704    0.71273    0.72884    0.74377    0.71353    0.71980    0.97626    1.05192


CASE NUMBER 10
ENTER ' &INPUT'
&INPUT  &END

CAV        VMAG     VPHA  ISMAG    ISPHA VPHA-ISPHA LS GAIN    POUT     EFF     PKE    PFW     PBW    PLC  PBAL ITER  SC
14 0.79821E 02  -0.8804 0.4880  -0.7046   0.1757   -4.7513    0.335  0.0004   -6.34  -0.66   -0.45   6.36 0.999    1   8
15 0.11820E 03   0.0246 0.5333   0.0313   0.0067    1.6274    1.455  0.0017   -7.95   0.46   -0.01   6.37 0.999    1   8
16 0.12490E 03   0.8008 0.5718   0.7649  -0.0359    5.4427    3.502  0.0041   -9.74   2.50   -0.34   6.40 0.999    1   8
17 0.15862E 03  -0.5250 0.6048  -0.5039   0.0211    8.1797    6.576  0.0078  -12.33   5.58   -0.92   6.44 0.999    1   8
18 0.23900E 03   0.2232 0.6295   0.2227  -0.0005   10.2913   10.694  0.0126  -16.89   9.70   -0.59   6.52 0.999    1   8
19 0.29491E 03  -0.9819 0.6474   0.9391   1.9210   11.9747   15.757  0.0186  -22.68  14.76   -0.02   6.65 0.998    1   8
20 0.30100E 03  -0.2187 0.6683  -0.3563  -0.1376   13.3442   21.598  0.0255  -28.32  20.60   -0.46   6.84 0.998    1   8
21 0.31790E 03   0.4856 0.6993   0.3401  -0.1455   14.4742   28.017  0.0331  -34.50  27.02   -1.04   7.09 0.998    1   8
22 0.38649E 03  -0.7939 0.7408  -0.9693  -0.1753   15.4068   34.728  0.0410  -42.23  33.73   -0.48   7.41 0.998    1   4
23 0.43524E 03  -0.0349 0.7956  -0.2839  -0.2490   16.1647   41.350  0.0488  -49.82  40.35   -0.07   7.82 0.998    1   2
24 0.42481E 03   0.7078 0.8675   0.4007  -0.3072   16.7723   47.558  0.0561  -55.82  46.56   -1.03   8.31 0.998    1   2
25 0.42182E 03  -0.5964 0.9473  -0.9106  -0.3143   17.2546   53.145  0.0627  -61.73  52.15   -1.46   8.88 0.997    1   1
26 0.42396E 03   0.1275 1.0254  -0.0878  -0.2153   17.9721   62.691  0.0740  -72.32  61.69   -1.16   9.50 0.997    1   1
27 0.50715E 03   0.9002 1.0609   0.8610  -0.0392   18.9972   79.381  0.0937  -89.96  78.38   -1.25  10.53 0.997    1   1
28 0.57927E 03  -0.3117 1.0626  -0.2027   0.1090   19.9034   97.801  0.1154 -109.16  96.80   -1.64  11.83 0.997    1   1
29 0.64221E 03   0.4888 1.0138   0.7186   0.2297   20.5126  112.527  0.1328 -124.95 111.53   -1.83  13.42 0.998    1   1
30 0.67489E 03  -0.6998 0.8913  -0.3738   0.3260   20.8040  120.338  0.1420 -134.56 119.34   -1.42  15.23 0.998    1   1
31 0.65640E 03   0.1088 0.6712   0.5242   0.4154   20.8298  121.055  0.1428 -137.57 120.06   -0.68  17.16 0.999    1   1
32 0.60222E 03   0.8944 0.3627  -0.5776  -1.4720   20.7069  117.678  0.1276  -61.49 116.68   -0.23  19.09 0.999    1   1
33 0.56428E 03  -0.3511 0.0547   0.4608   0.8119   20.5986  114.778  0.1244  -60.49 113.78   -0.18  20.98 0.999    1   1
34 0.57848E 03   0.3971 0.2180   0.1895  -0.2076   20.6684  116.638  0.1264  -64.29 115.64   -0.22  22.82 0.999    1   1
35 0.61486E 03  -0.8384 0.3604  -0.9224  -0.0840   20.8797  122.453  0.1327  -72.02 121.46   -0.16  24.68 0.999    1   1
36 0.63728E 03  -0.0638 0.3421  -0.0929  -0.0291   21.0816  128.279  0.1391  -79.86 127.28   -0.05  26.64 0.999    1   1
37 0.63746E 03   0.7089 0.2067   0.5978  -0.1111   21.1639  130.734  0.1417  -84.35 129.74    0.00  28.69 0.999    1   1

NORMALIZED VELOCITIES
   1.11769    1.08871    1.06170    1.03506    1.05526    1.05811    1.03324    0.98214    0.99126    0.99719    0.98395    0.97967
   0.98538    0.99306    0.94213    0.85812    0.75699    0.71273    0.72882    0.74377    0.71353    0.71977    0.97628    1.05191


CASE NUMBER 11
ENTER ' &INPUT'
```

Figure 7. - Concluded.

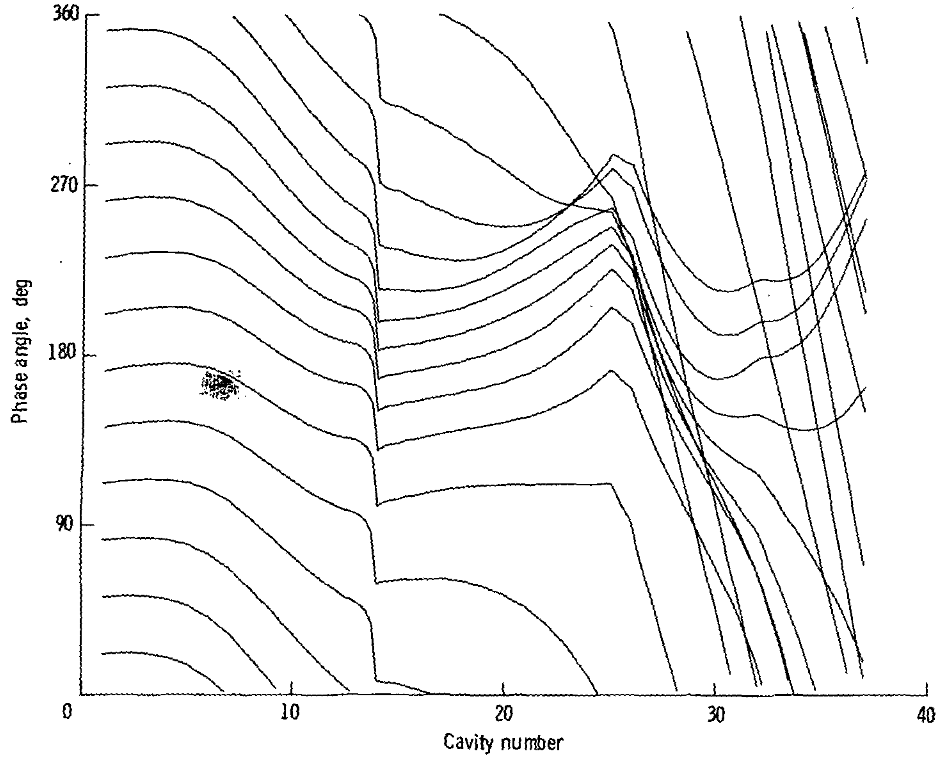

Figure 8. - Applegate diagram for sample case.

REFERENCES

1. Kosmahl, Henry G.: A Novel, Axisymmetric, Electrostatic Collector for Linear Beam Microwave Tubes. NASA TN D-6093, 1971.

2. Sauseng, O. G.: Applied Research on Efficiency Improvement in O-Type Traveling-Wave Tubes. Hughes Aircraft Co. (RADC-TR-67-259; AD-818085), 1967.

3. Stankiewicz, N.: Evaluation of Magnetic Refocusing in Linear-Beam Microwave Tubes. NASA TN D-7660, 1974.

4. Connolly, Denis J.; and O'Malley, Thomas A.: Computer Program for Analysis of Coupled-Cavity Traveling-Wave Tubes. NASA TN D-8492, 1977.

5. Vaughan, J. Rodney M.: Calculation of Coupled-Cavity TWT Performance. IEEE Trans. Electron Devices, vol. ED-22, No. 10, Oct. 1975, pp. 880-890.

6. Kino, G. S.; et al.: Small-Signal and Large-Signal Theories for the Coupled Cavity TWT. Proceedings of the Sixth International Conference on Microwave and Optical Generation and Amplification. Inst. Electr. Eng., 1966, pp. 49-53.

7. Tien, P. K.; Walker, L. R.; and Wolontis, V. M.: A Large Signal Theory of Traveling-Wave Amplifiers. Proc. IRE, vol. 43, no. 3, Mar. 1955, pp. 260-277.

8. Gewartowski, James W.; and Watson, H. A.: Principles of Electron Tubes, Including Grid-Controlled Tubes, Microwave Tubes and Gas Tubes. Van Nostrand, 1965.

"The aeronautical and space activities of the United States shall be conducted so as to contribute . . . to the expansion of human knowledge of phenomena in the atmosphere and space. The Administration shall provide for the widest practicable and appropriate dissemination of information concerning its activities and the results thereof."

—NATIONAL AERONAUTICS AND SPACE ACT OF 1958

NASA SCIENTIFIC AND TECHNICAL PUBLICATIONS

TECHNICAL REPORTS: Scientific and technical information considered important, complete, and a lasting contribution to existing knowledge.

TECHNICAL NOTES: Information less broad in scope but nevertheless of importance as a contribution to existing knowledge.

TECHNICAL MEMORANDUMS: Information receiving limited distribution because of preliminary data, security classification, or other reasons. Also includes conference proceedings with either limited or unlimited distribution.

CONTRACTOR REPORTS: Scientific and technical information generated under a NASA contract or grant and considered an important contribution to existing knowledge.

TECHNICAL TRANSLATIONS: Information published in a foreign language considered to merit NASA distribution in English.

SPECIAL PUBLICATIONS: Information derived from or of value to NASA activities. Publications include final reports of major projects, monographs, data compilations, handbooks, sourcebooks, and special bibliographies.

TECHNOLOGY UTILIZATION PUBLICATIONS: Information on technology used by NASA that may be of particular interest in commercial and other non-aerospace applications. Publications include Tech Briefs, Technology Utilization Reports and Technology Surveys.

Details on the availability of these publications may be obtained from:

SCIENTIFIC AND TECHNICAL INFORMATION OFFICE

NATIONAL AERONAUTICS AND SPACE ADMINISTRATION

Washington, D.C. 20546